



www.sciencemag.org/cgi/content/full/323/5910/112/DC1

Supporting Online Material for

Control of Self-Assembly of DNA Tubules Through Integration of Gold Nanoparticles

Jaswinder Sharma, Rahul Chhabra, Anchi Cheng, Jonathan Brownell, Yan Liu,*
Hao Yan*

*To whom correspondence should be addressed. E-mail: hao.yan@asu.edu (H.Y.); yan_liu@asu.edu (Y.L.)

Published 2 January 2008, *Science* **323**, 112 (2008)
DOI: 10.1126/science.1165831

This PDF file includes:

Materials and Methods
SOM Text
Figs. S1 to S21
Table S1

Other Supporting Online Material for this manuscript includes the following:
(available at www.sciencemag.org/cgi/content/full/323/5910/112/DC1)

Movies S1 to S7

Supporting Online Material

Control of Self-Assembly of DNA Tubules Through Integration of Gold Nanoparticles

Jaswinder Sharma, Rahul Chhabra, Anchi Cheng, Jonathan Brownell, Yan Liu, Hao Yan

Materials and Methods

Materials. All DNA strands, unmodified and modified with disulfide functionality, were purchased from Integrated DNA Technologies, Inc. (www.IDTDNA.com) and purified by denaturing polyacrylamide gel electrophoresis (PAGE). DNA strands were quantified by measuring the optical density at 260 nm wavelength. Colloidal solution of different sized Gold nanoparticles (AuNps) was purchased from Ted Pella Inc. Bis(p-sulfonatophenyl)phenylphosphine dihydrate dipotassium salt (BSPP) was purchased from Strem Chemicals Inc.

Phosphination of AuNPs. BSPP (40 mg) was mixed with citrate ion stabilized AuNps (100 mL) and the mixture was stirred overnight for ligand exchange. Phosphine ligands incur enhanced stability against higher electrolyte concentration. NaCl (solid) was added slowly with continuous stirring until the color of the solution changed from deep burgundy to purple. The mixture was centrifuged at 3000 rpm for 30 minutes and the supernatant was removed carefully. AuNp pellets were resuspended in 1 mL BSPP solution (2.5 mM). The AuNps were further washed with 1 mL methanol and centrifuged again to collect AuNps. Finally, the AuNps were resuspended in 1 mL BSPP solution (2.5 mM) and quantified by measuring the optical absorbance at ~ 520 nm wavelength. The method of phosphine ligand exchange is general and can be applied to any sized AuNps.

Preparation of AuNP-DNA conjugates with discrete copies of DNA. Disulfide-modified DNA strands were incubated with equimolar ratios of phosphinated AuNps in 0.5xTBE buffer (89 mM Tris, 89 mM boric acid, 2 mM EDTA, pH 8.0) containing 50 mM NaCl overnight at room temperature. AuNp-DNA conjugates carrying discrete copies of DNA were separated by 3% agarose gel (running buffer 0.5xTBE, loading buffer 50% glycerol, 15 V/cm). The desired band, comprised of a 1:1 ratio of AuNp-DNA conjugates, was electroeluted into a glass fiber filter membrane supported by dialysis membrane (MWCO 10000). AuNp-DNA conjugates were recovered using a 0.45 μ m centrifugal filter device. AuNp-DNA conjugates were quantified using optical absorbance at ~ 520 nm. The 1:1 AuNp-DNA conjugates were further stabilized with short disulfide-modified oligonucleotides T₅-ssDNA ([HS-T₅]/[AuNP]=100, in 0.5xTBE, 50 mM NaCl) and incubated for 12 hrs at room temperature. Short DNA components provide additional stability against higher electrolyte concentration necessary for DNA self-assembly. AuNps-DNA conjugates with different sized AuNps were prepared using the same method.

Assembly of DNA tube like architectures. DNA tubes were formed by mixing equimolar quantities of all the constituent strands at 100 nM (Figure S1) in 1xTBE buffer (89 mM Tris, 89 mM boric acid, 2 mM EDTA, 400 mM NaCl, pH 8.0). Note that the unmodified DX-A3 and/or DX-C3 strands were replaced by 1:1 AuNp-DNA conjugates and the mixture was cooled slowly from 65 °C to room temperature over 24 hours.

TEM analysis. The TEM sample was prepared by depositing (3 μ L) of DNA tubes on carbon-coated grid (400 mesh, Ted pella). Before depositing the sample, the grids were glow discharged using an Emitech K100X machine. After deposition, the excess sample was wicked from the grid with a piece of filter paper. The grid was washed with water by touching it quickly with a drop of water and wicking out the excess with filter paper. TEM images were collected using a Philips CM12 transmission electron microscope, operated at 80 kV in the bright field mode.

AFM imaging. DNA arrays samples (2 μ L) were deposited onto a freshly cleaved mica (Ted Pella, Inc.) and left to adsorb for 3 min. Buffer (1 x TAE-Mg²⁺, 400 μ L) was added to the liquid cell and the sample was scanned in a tapping mode on a Pico-Plus AFM (Molecular Imaging, Agilent Technologies) with NP-S tips (Veeco, Inc.).

Cryo-EM imaging and tomography: Nanotubes embedded in vitreous ice were imaged in area free of carbon support at liquid nitrogen temperature. The electron tomography data was collected on microscope with FEG or tungsten filament electron gun at 120 kV. Leginon was used to track the targeting area to collect images on 2k or 4k CCDs [C. Suloway *et al.*, *J. Struct. Biol.* **151**, 41 (2005) and C. Suloway *et al.*, *Submitted*). The tilts series were at 2 degree increment and extended up to +/- 60 degree whenever possible. Due to limitation in goniometer movement imposed by the cryo-specimen holder dimension, most tilt series did not span the full range. In addition, the beam-induced movement at high tilts were strong in most data collection as can be seen in the tilt series movie presented in the supplementary material. As a result, the gold beads reconstructed are strongly oblong and noisier than ideal.

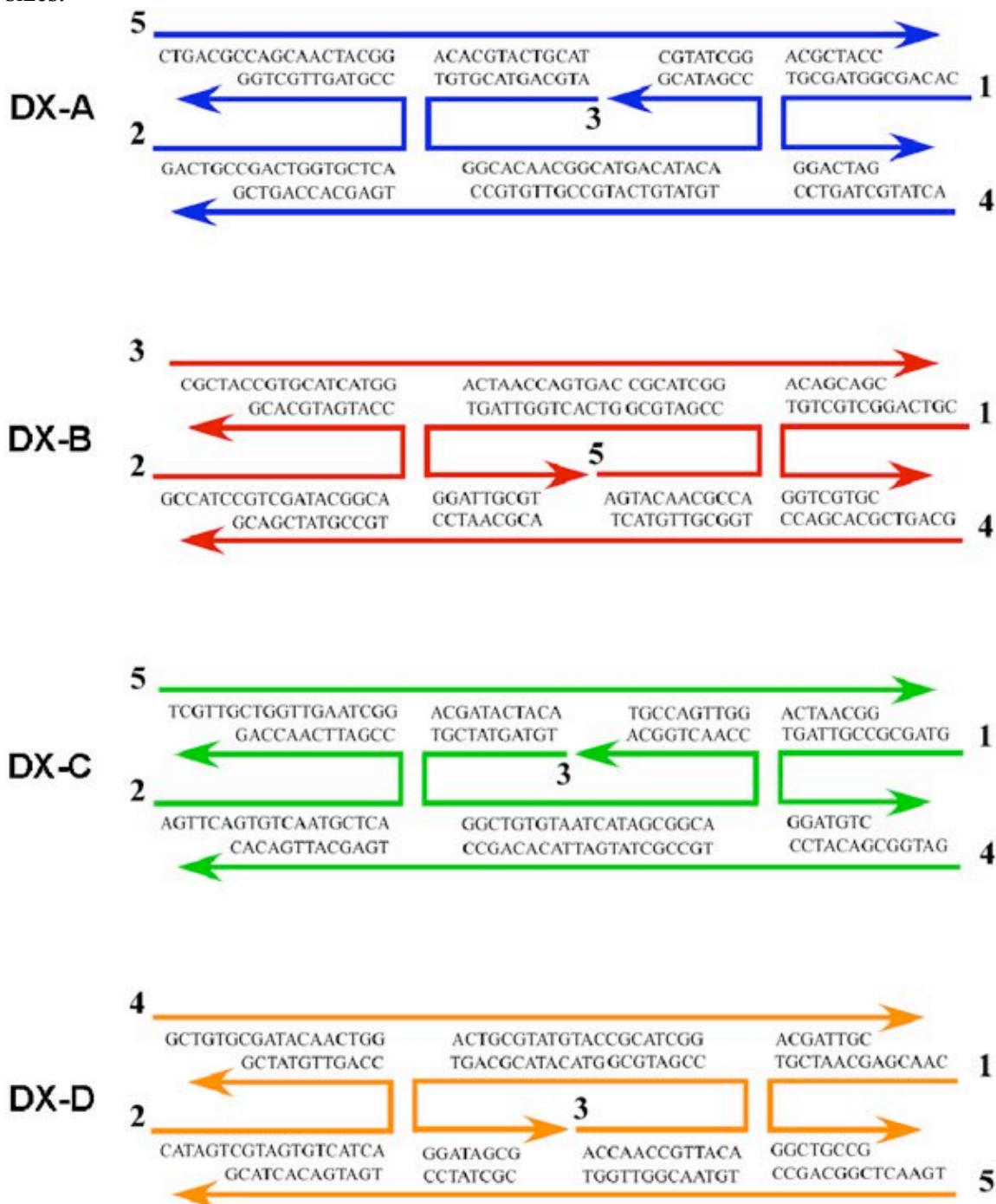
IMOD [J. R. Kremer, D. N. Mastronarde, J. R. McIntosh, *J. Struct. Biol.* **116**, 71 (1996).] was used for the tomographic reconstruction with isolated free gold clusters as fiducials. In some cases, Gaussian and bandpass filtering were necessary to remove the noise. The cropped and down-sampled tomograms were examined and the surface rendered blobs colored in UCSF Chimera [E. F. Pettersen *et al.*, *J. Comput. Chem.* **25**, 1605 (2004).].

It should be pointed out that even with the protection of vitreous ice, the tubes imaged were not perfectly round. Larger tubes in particular tend to be flat on one side (See Movies in the Supplementary Material). It was likely that the tubes interacted preferentially with the air-water interface.

Comment on the thermo-stability of 3D DNA tubules with AuNPs. From the previous work done by Mirkin *et al.* (*Science* **1997**, 277, 1078-1081, *J. Am. Chem. Soc.* **2003**, 125, 1643-1654; *Anal. Chem.* **2007**, 79, 7201-7205 and references cited therein), Rotello *et al.* (*Chem. Biol. Drug Des.* **2006**, 67, 78-82) and others, it has been concluded that melting temperatures of the DNA conjugated to AuNPs are higher than that of the DNA alone. We anticipate that these 3D DNA tubules carrying AuNPs may have higher thermodynamic stability in contrast to DNA only tubules, such effect will need more systematic studies in the future.

Supporting Figures and Tables

Figure S1. DNA sequences used in the assembly of DNA tubes. DNA tubes were prepared by mixing 1:1 AuNps-DNA conjugates with the other constituting unmodified DNA strands as shown below. The DX-A3 and/or DX-C3 strands were replaced by 1:1 AuNps-DNA conjugates to yield DNA tubes with different conformations and AuNp sizes.



DNA sequences of DX-A3 and DX-C3 with loop and spacers. A spacer is a short DNA sequence between the random custom-designed DNA sequences and the disulfide modification. Note that to conjugate disulfide-modified DNA with 5 nm AuNps, 50-mer DNA was used. In contrast, to conjugate DNA with 10 nm and 15 nm AuNps, 100-mer DNA strands were used to aid in the gel separation protocol. The required length of DNA was achieved by adding free thymine residues at one end of the custom-designed DNA strand.

A3- (100)

5'-SSH-

TTTTTATGCAGTACGTGTGGCACAACGGCATGACATACACCGATACGTTTTTT
TT-3'

A3- (50)

5'-SSH-

TTTTTTTTATGCAGTACGTGTGGCACAACGGCATGACATACACCGATACG-3'

C3 (100)

5'-SSH-

TTTTTAGTATCGTGGCTGTGTAATCATAGCGGCACCAACTGGCATGTTTTTTTT
TT-3'

C3 (50)

5'-SSH-

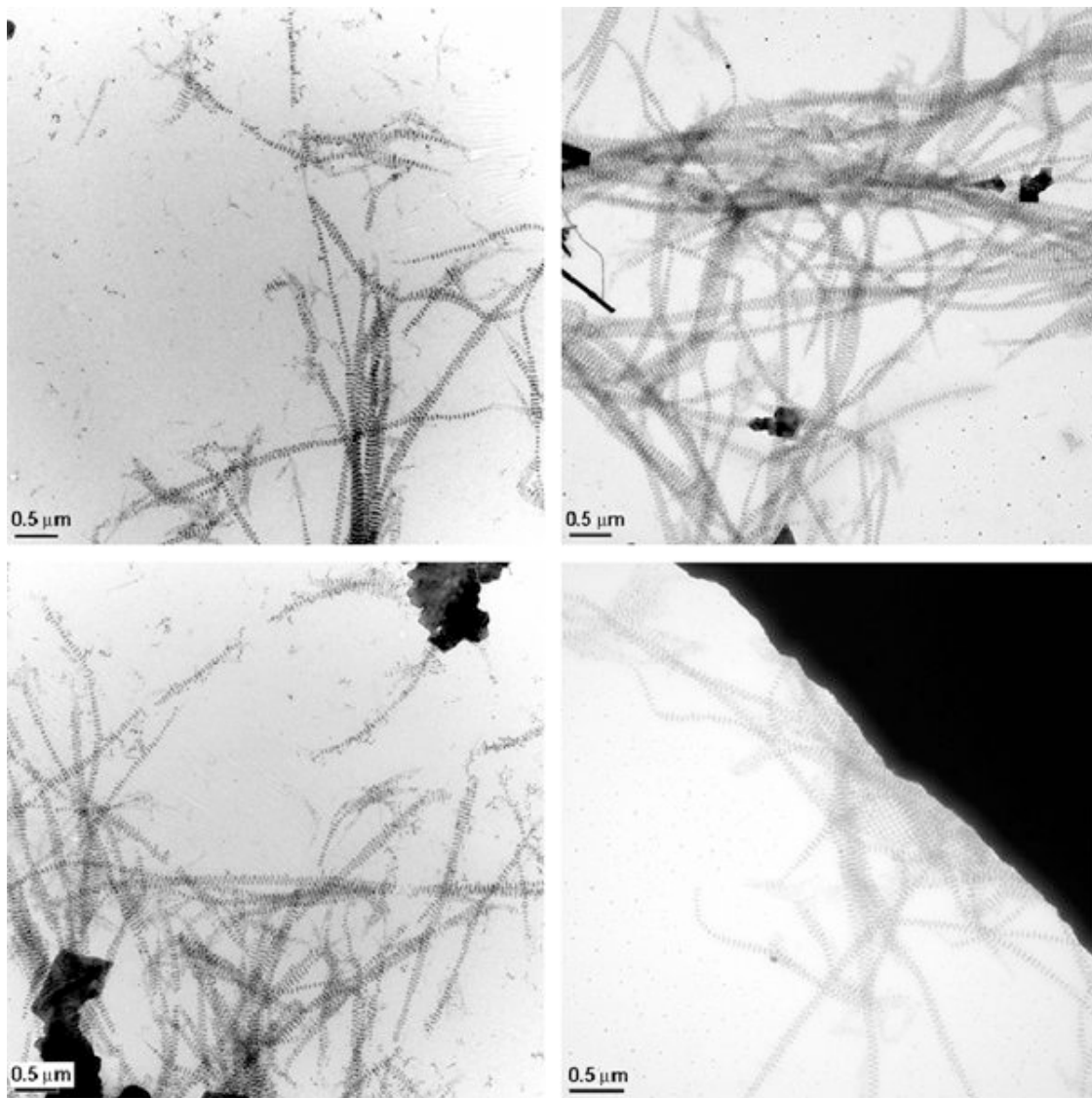
TTTTTTTTAGTACGTGTGGCACAACGGCATGACATACACCGATACGATGC-3'

C3-with stem loop

5'-

CATGTAGTATCGTGGCTGTGTAATCATTTTTTTTTTTTTTTTTTTTTTTTTTTTAGC
GGCACCAACTGG-3'

Figure S2. Additional zoom-out images of DNA tubes with 5 nm AuNps in the A-tile and a random DNA loop in the C-tile.



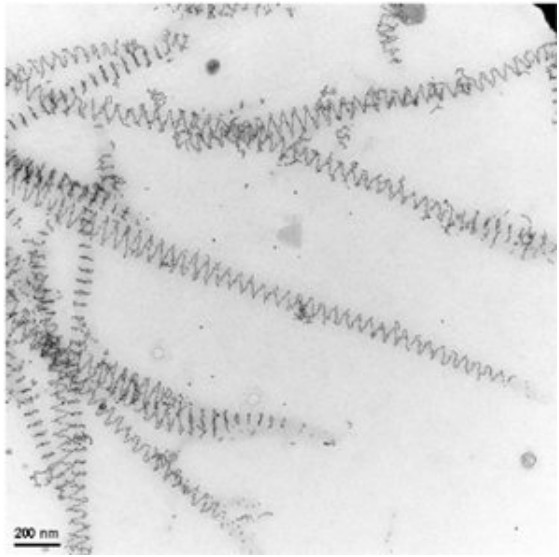
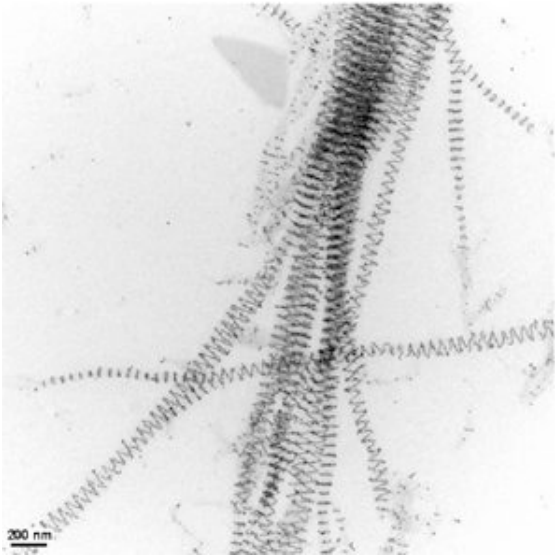
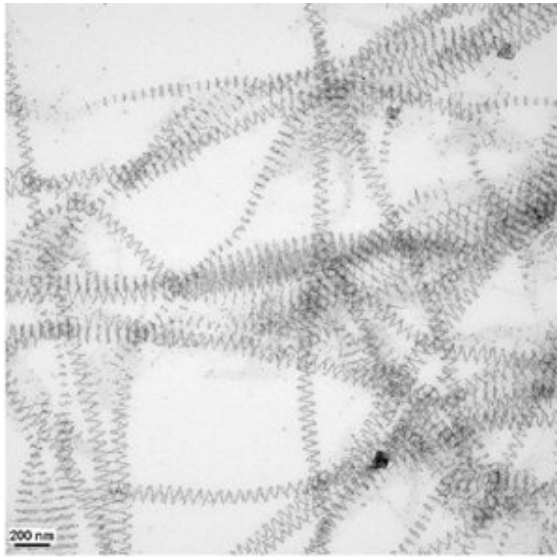
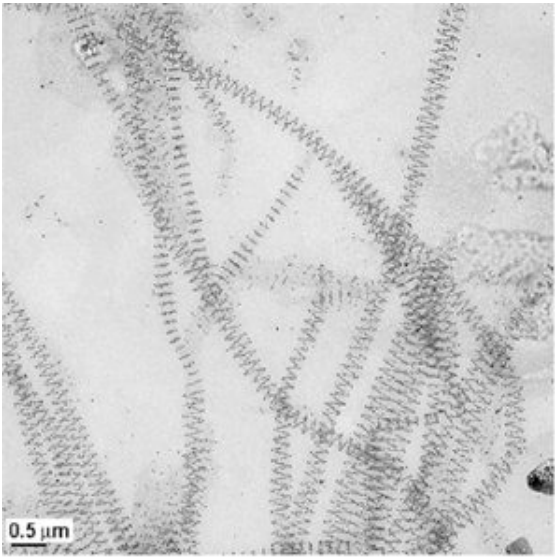
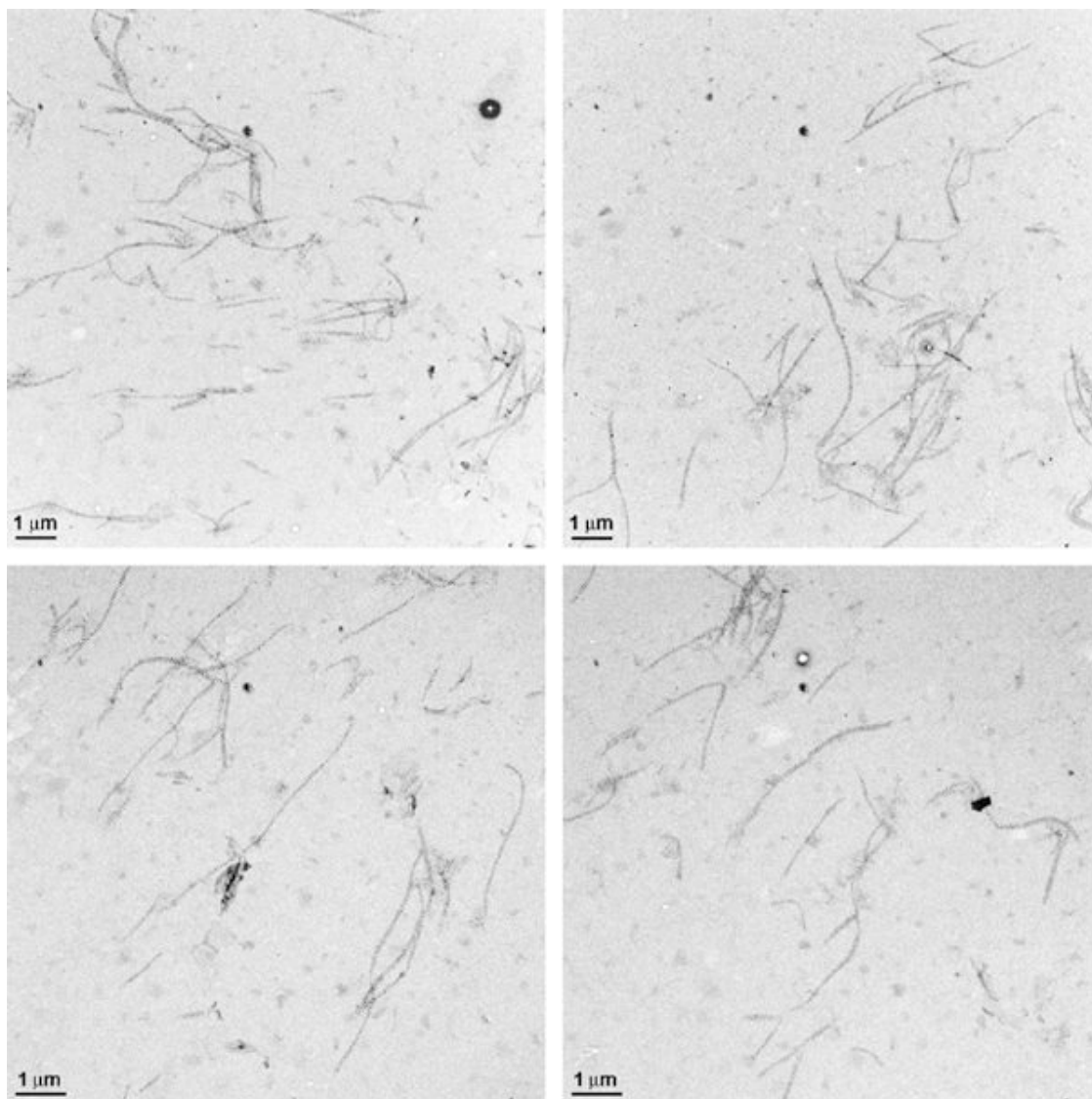


Figure S3. Additional zoom-out images of DNA tubes with 5 nm AuNps in the A-tile.



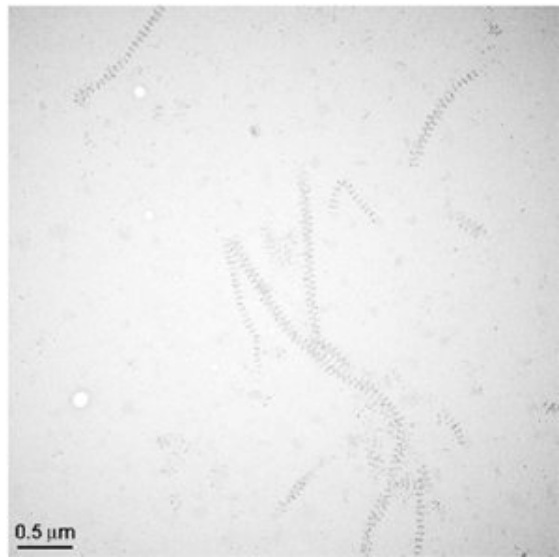
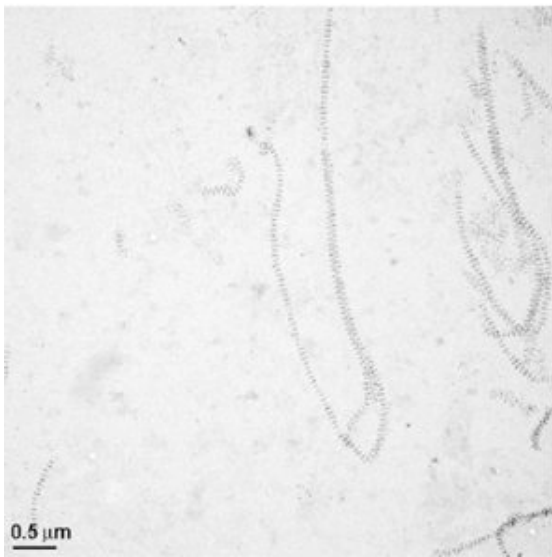
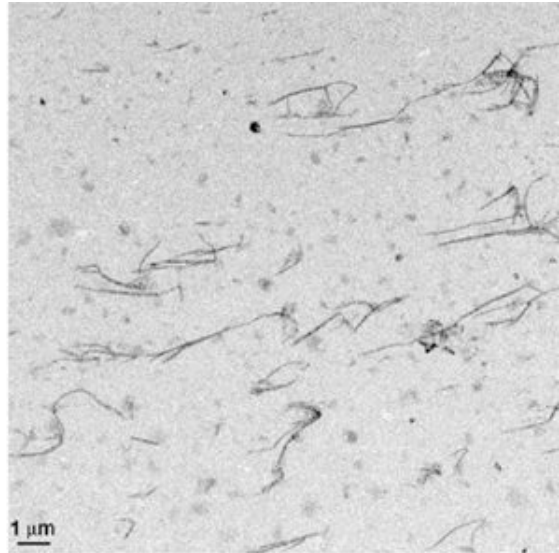
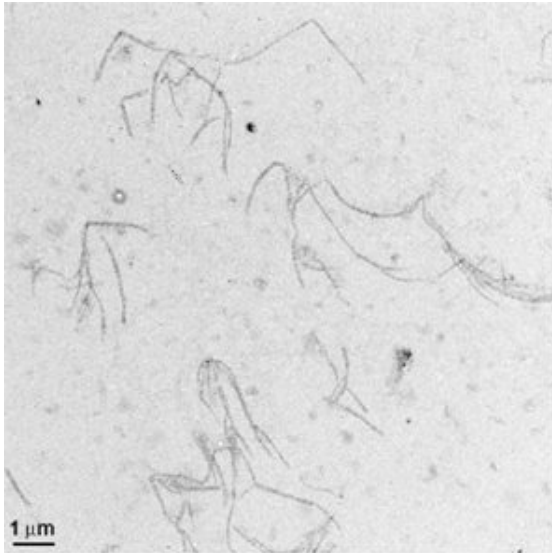
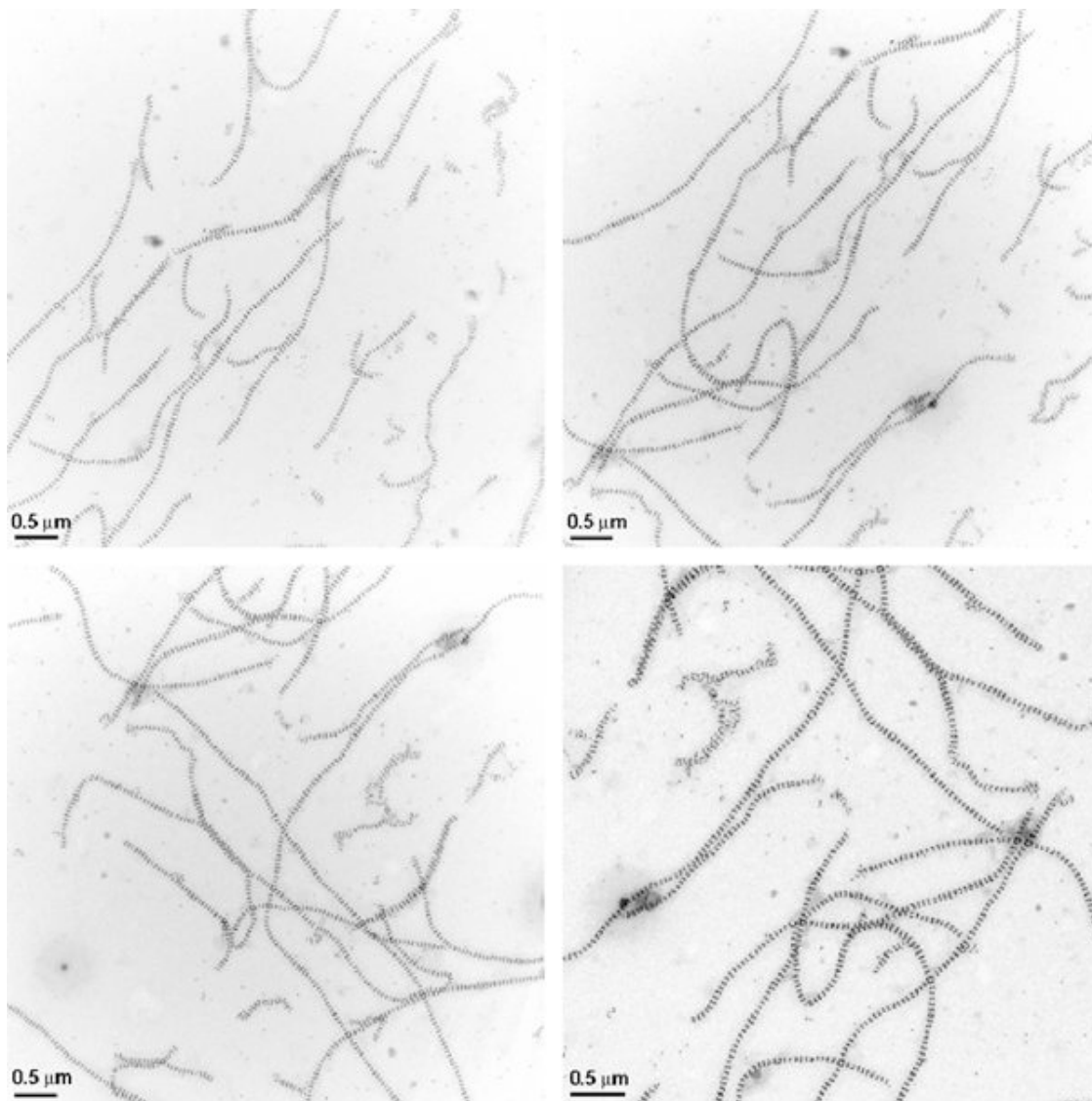


Figure S4. Additional zoom-out images of DNA tubes with 10 nm AuNps in the A-tile. It is obvious that most tubes are stacked ring structures.



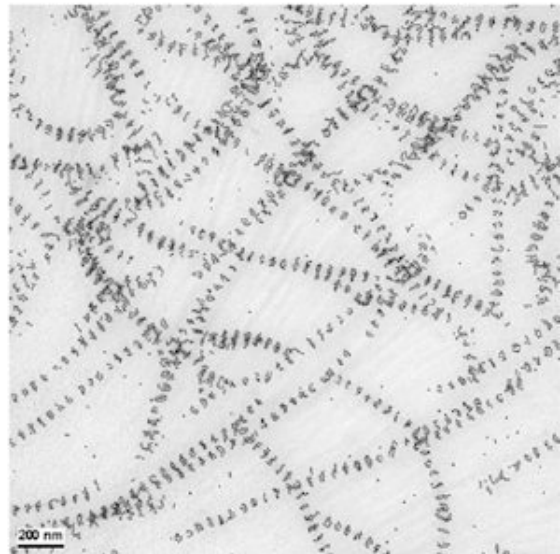
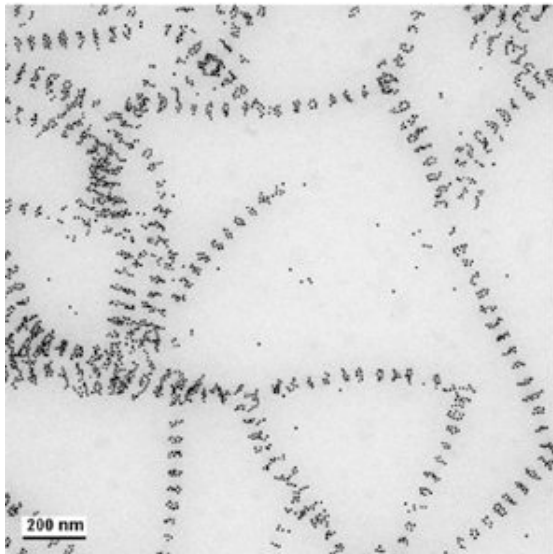
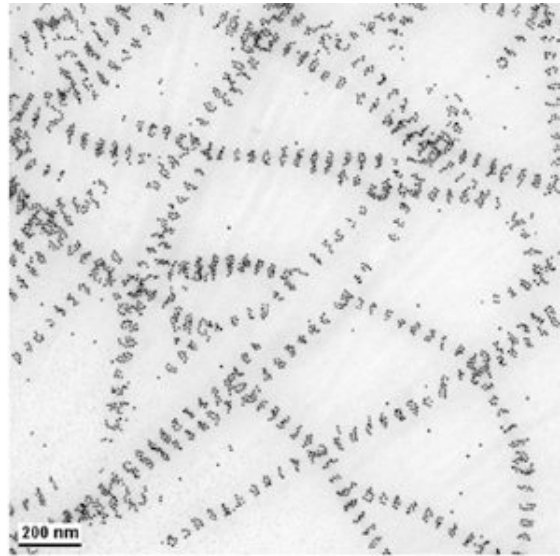
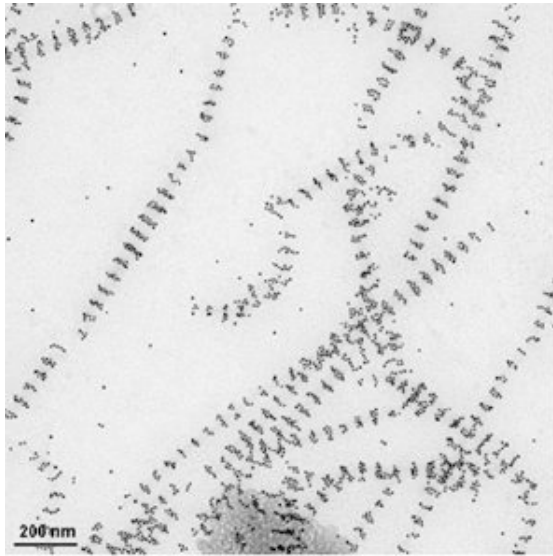
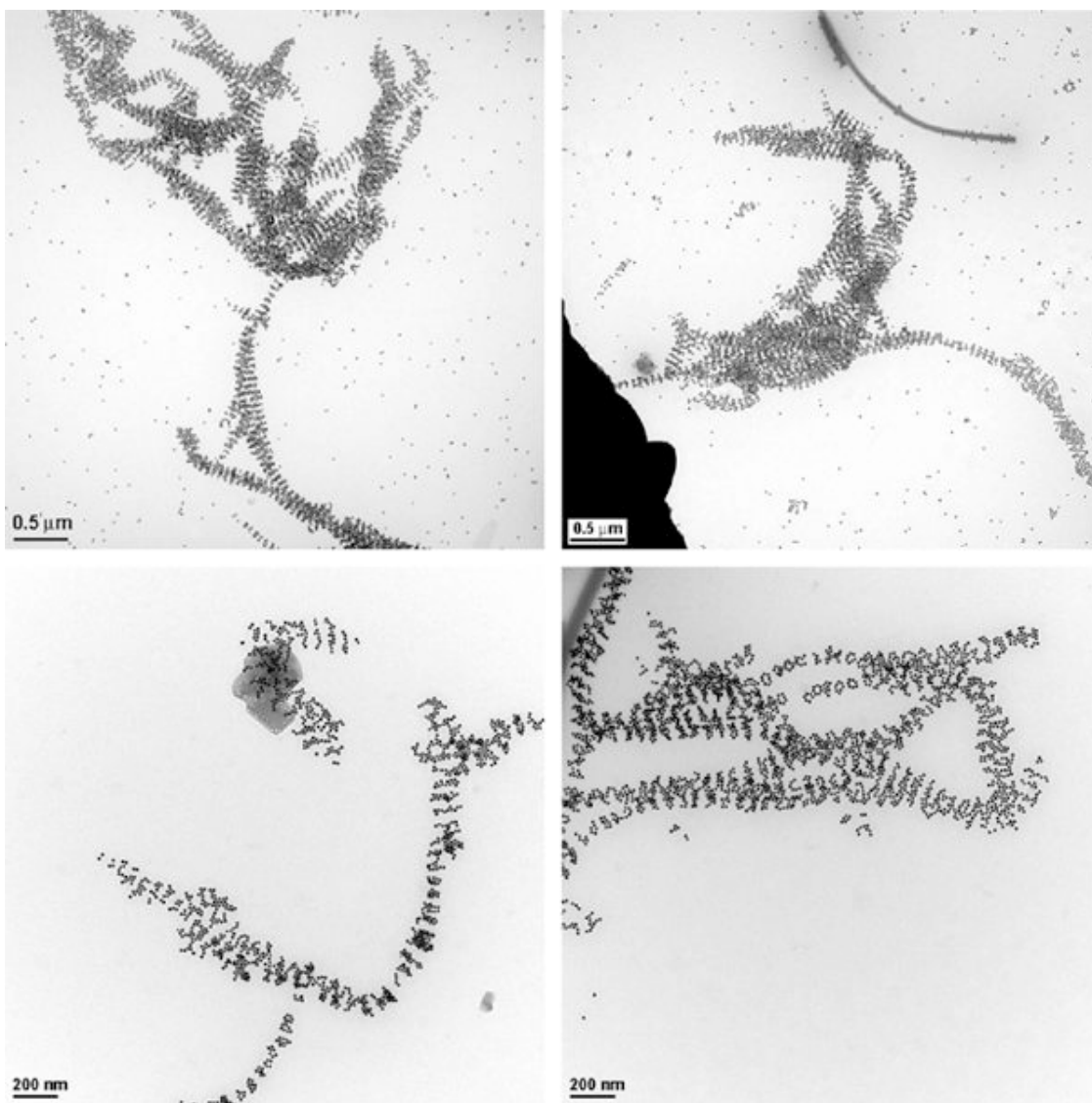


Figure S5. Additional zoom-out images of DNA tubes with 15 nm AuNps in the A-tile.



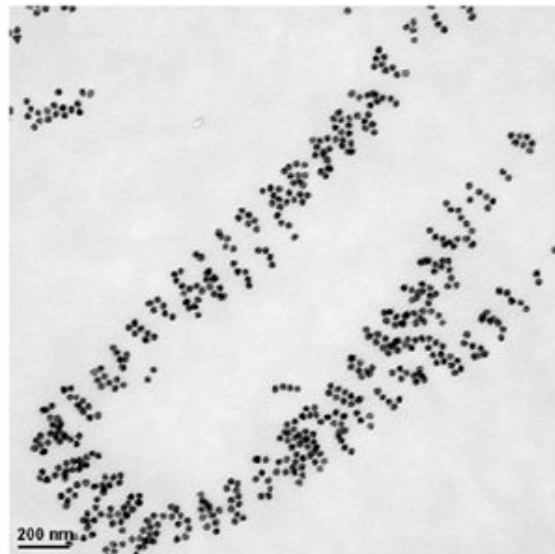
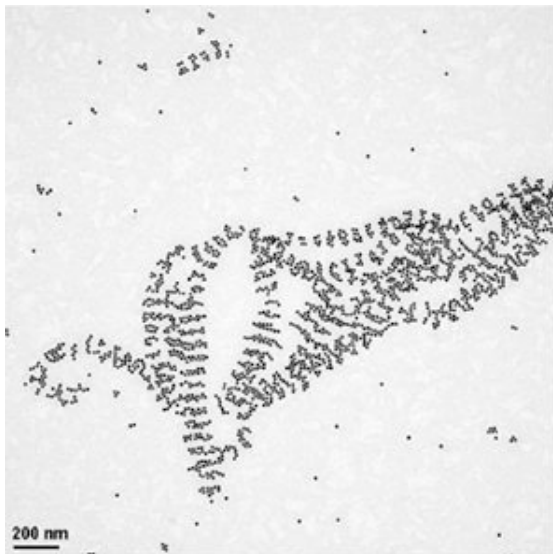
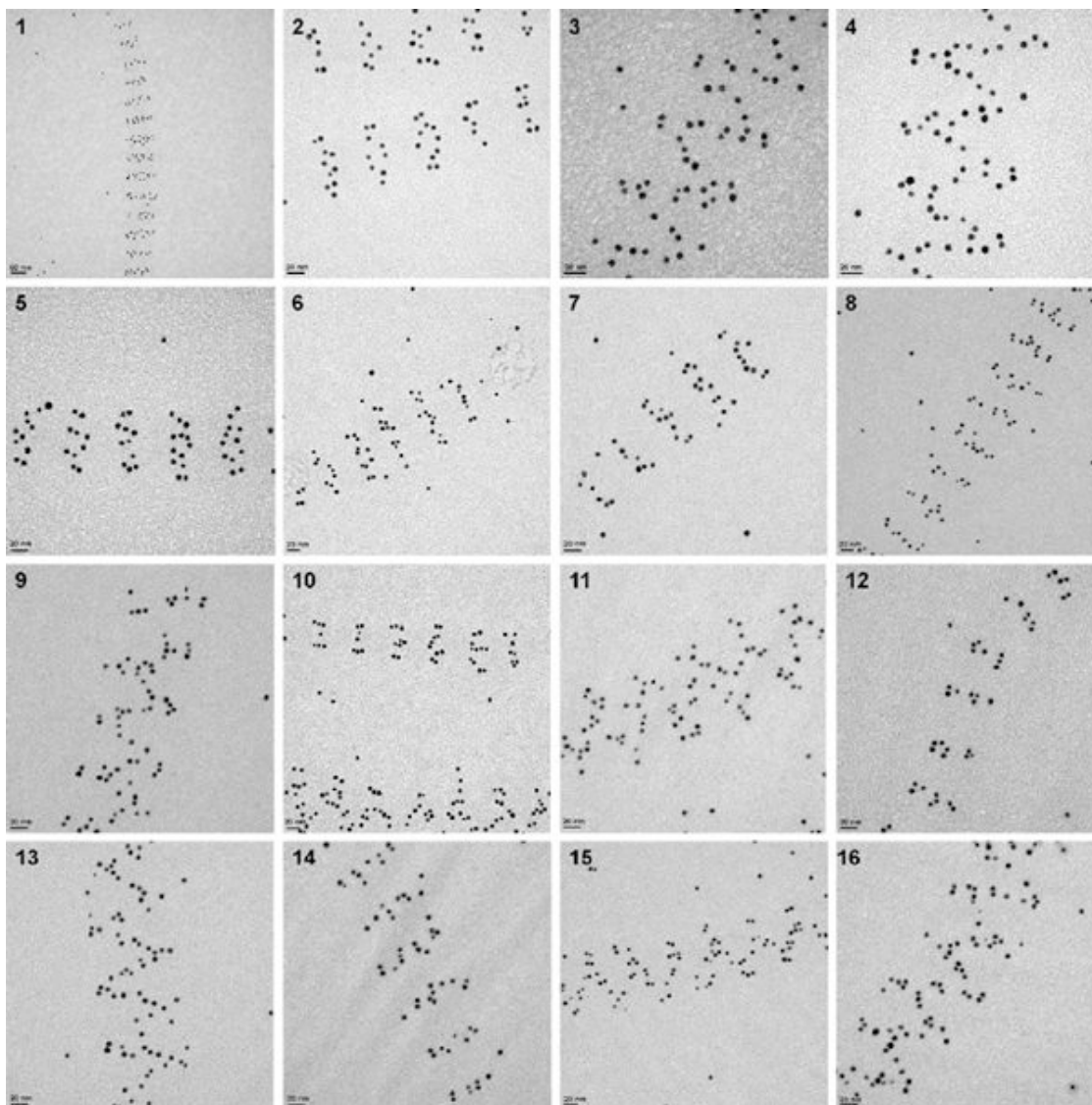
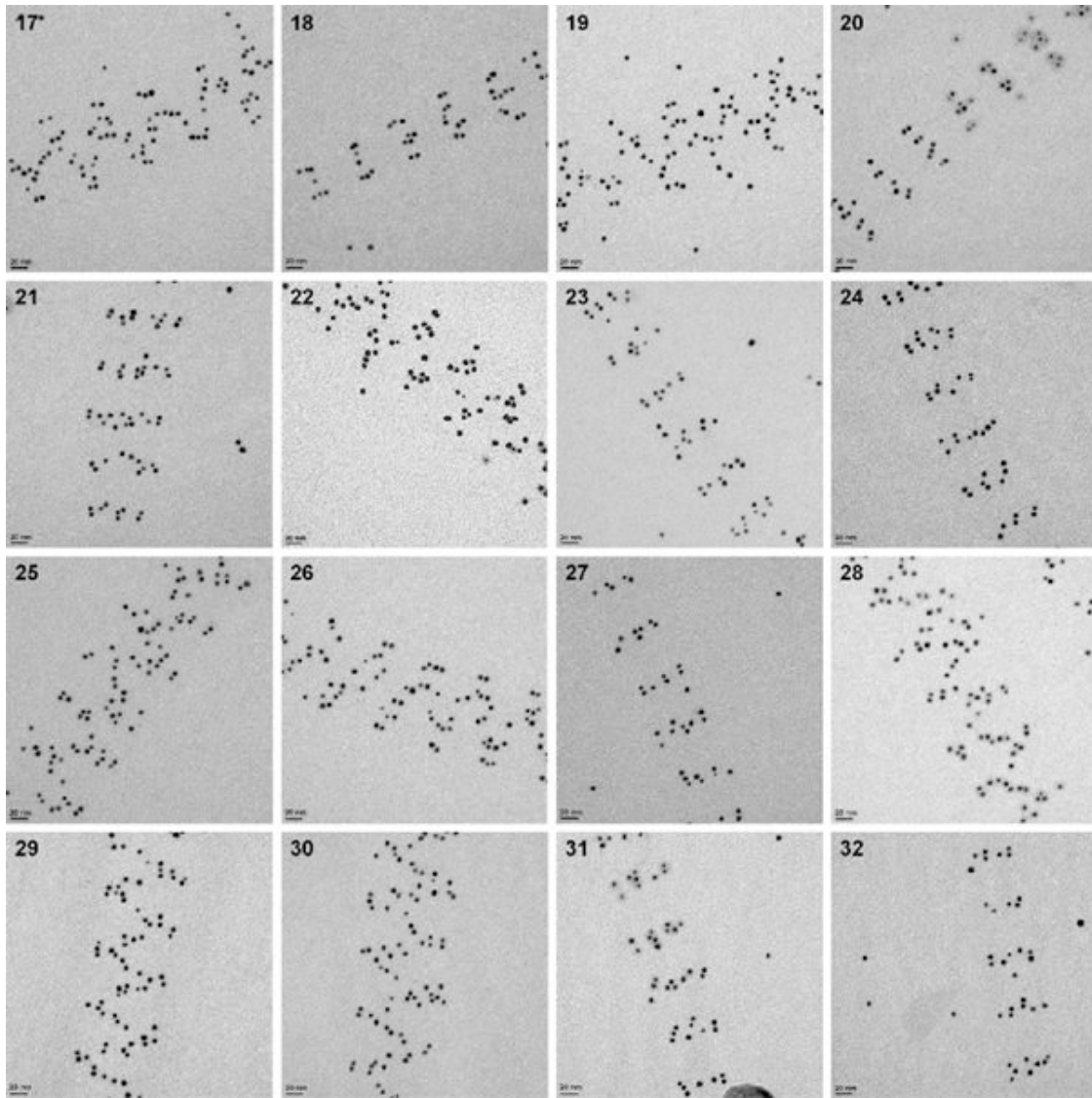
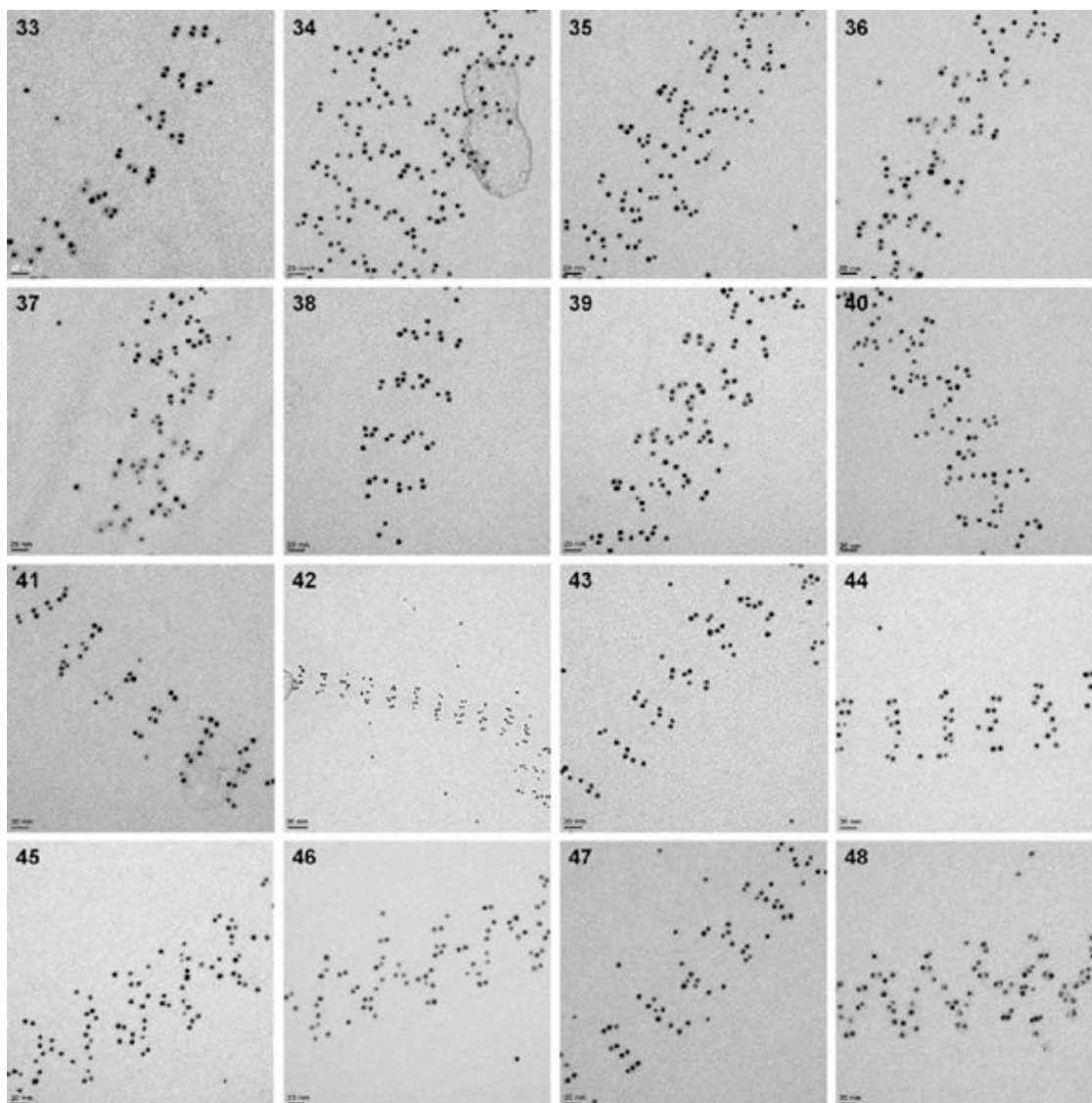
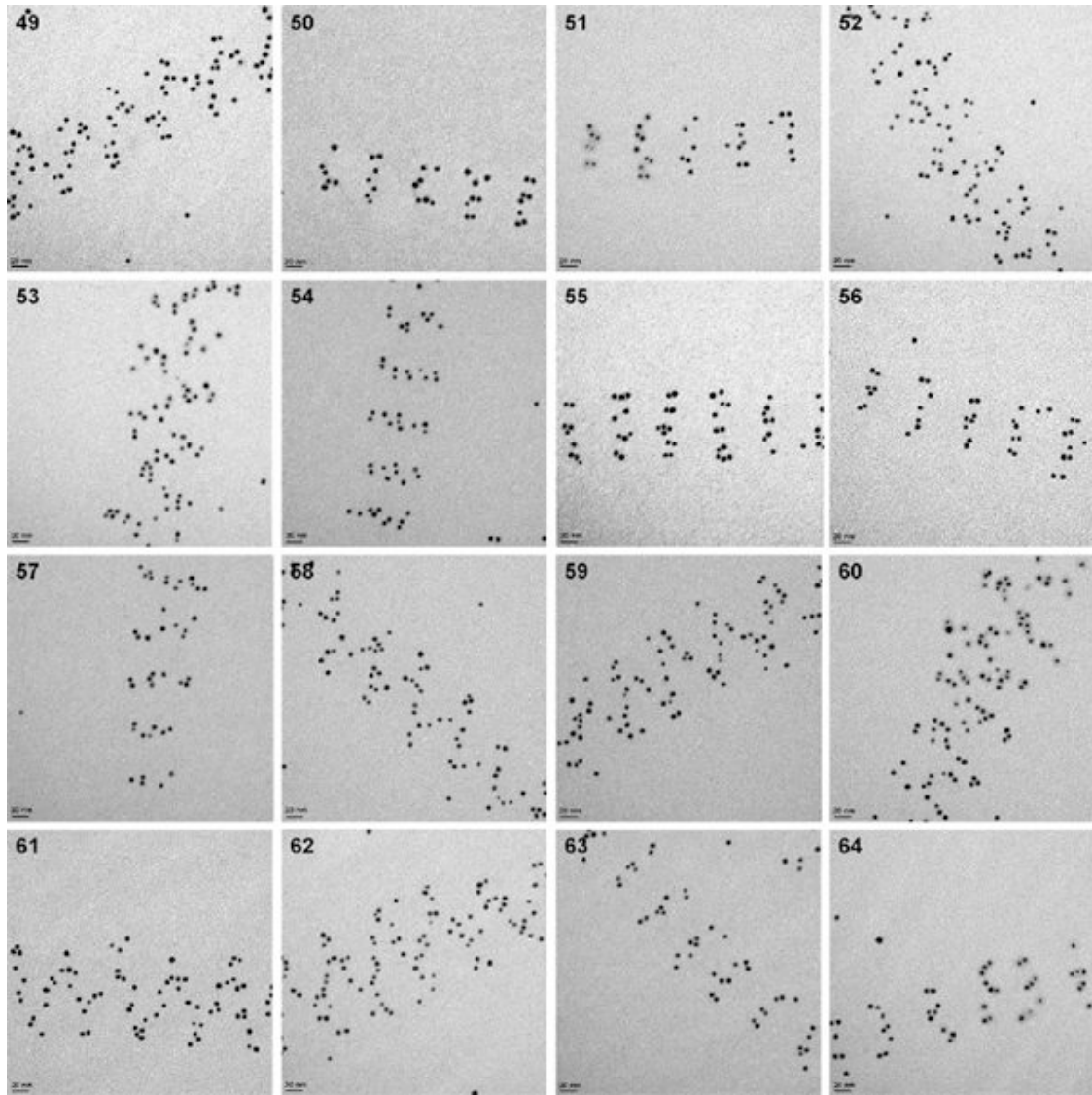


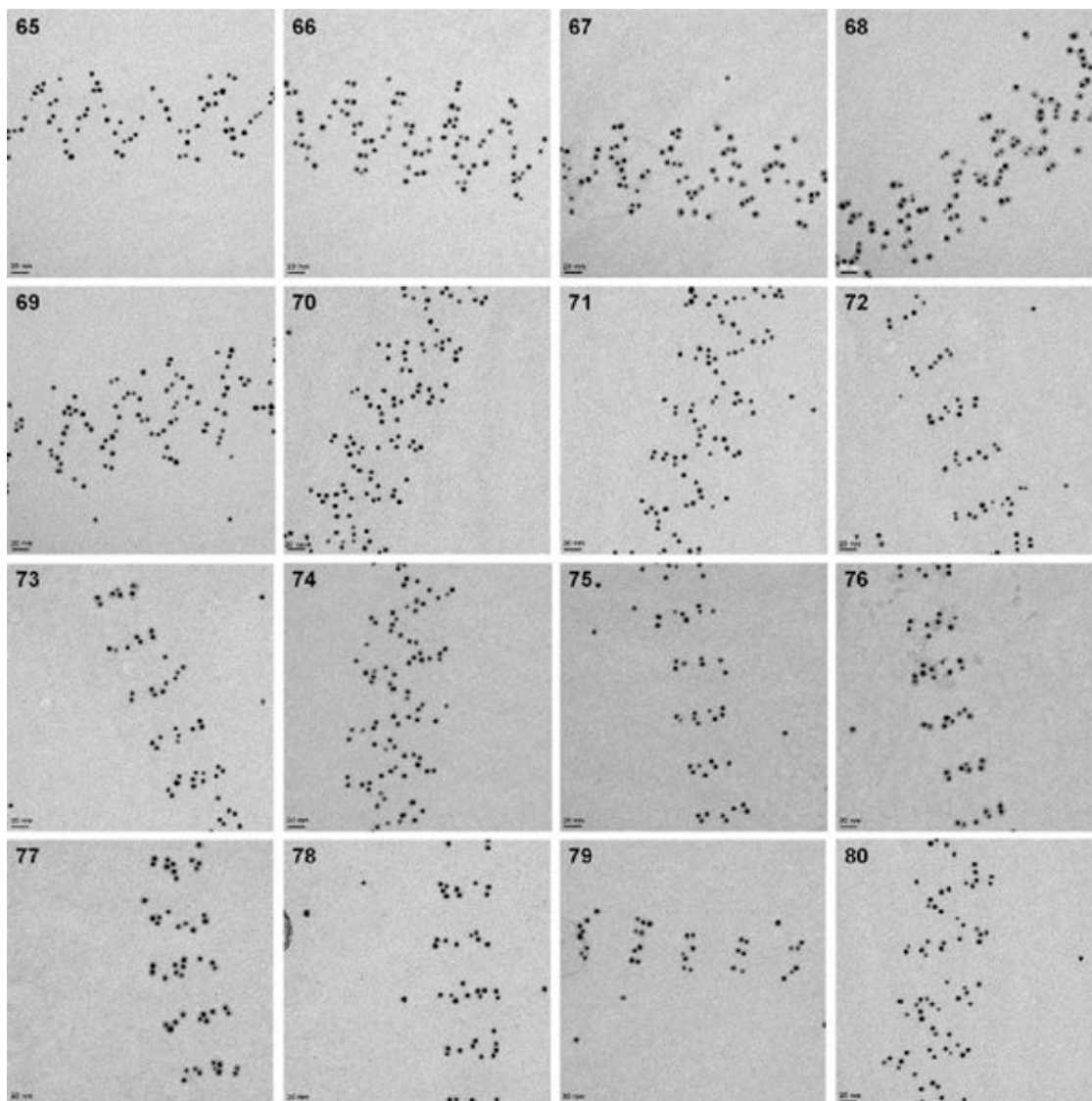
Figure S6. Additional zoom-in TEM images of DNA tubes with 5 nm AuNps in the A-tile used in the statistical analysis.











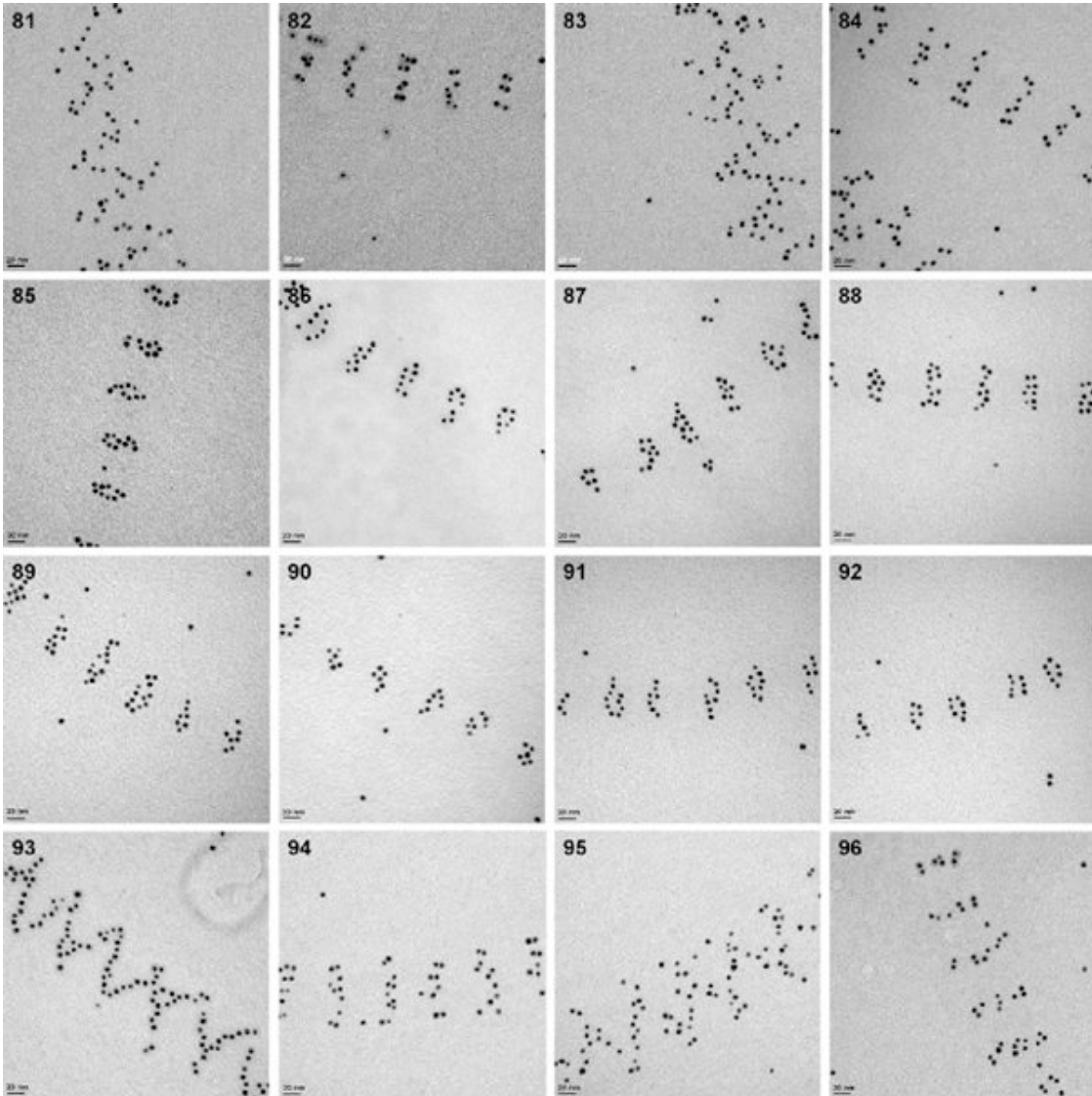
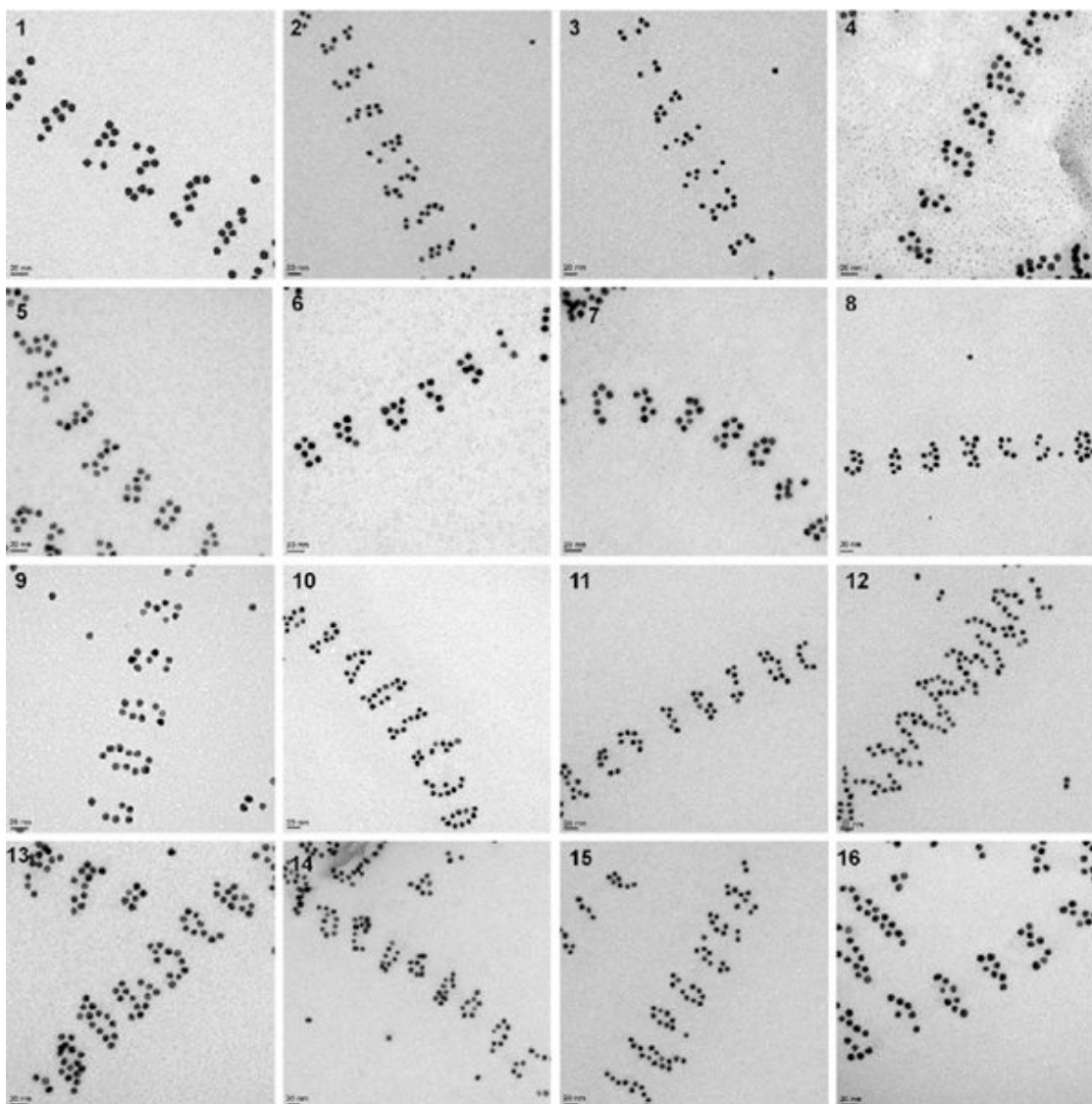
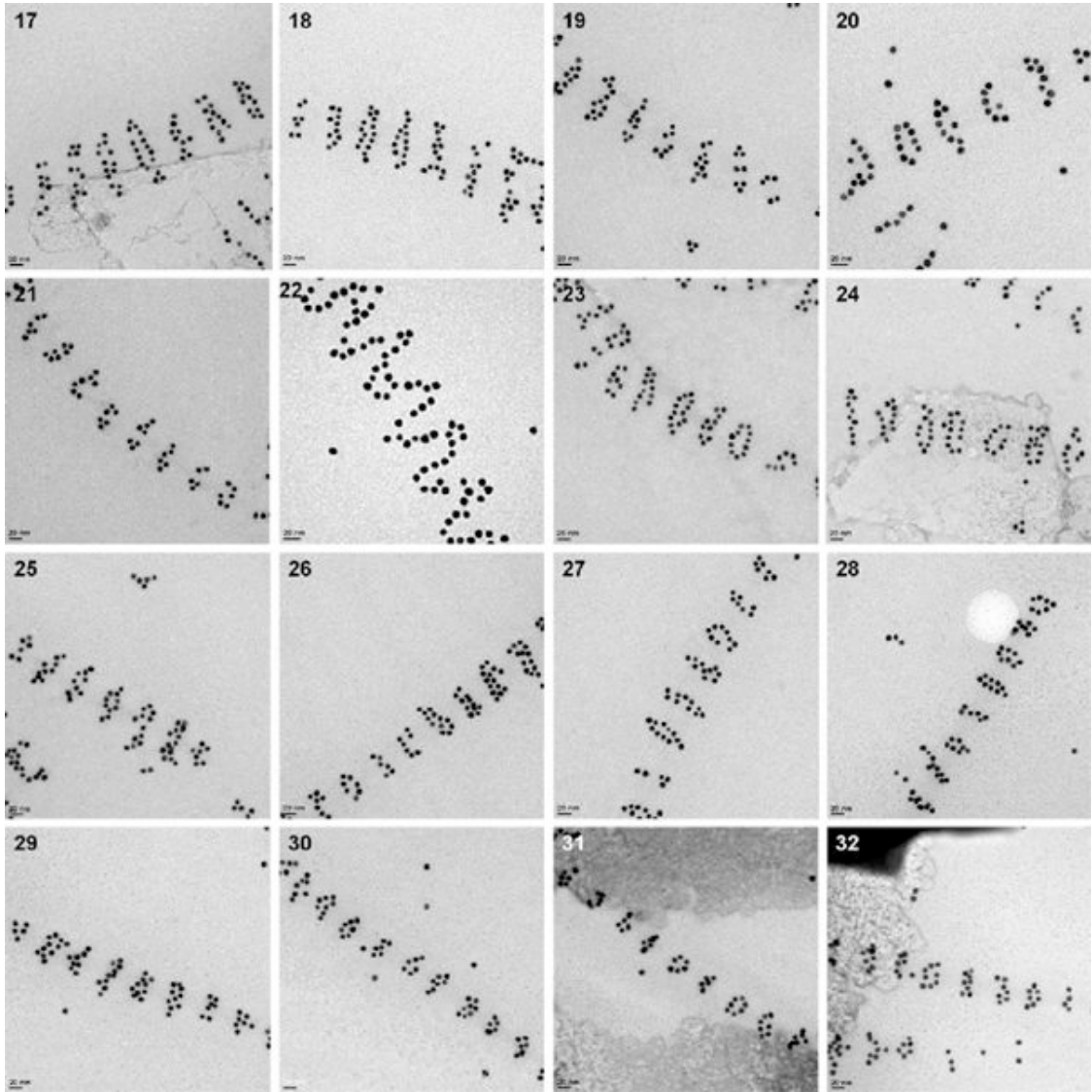
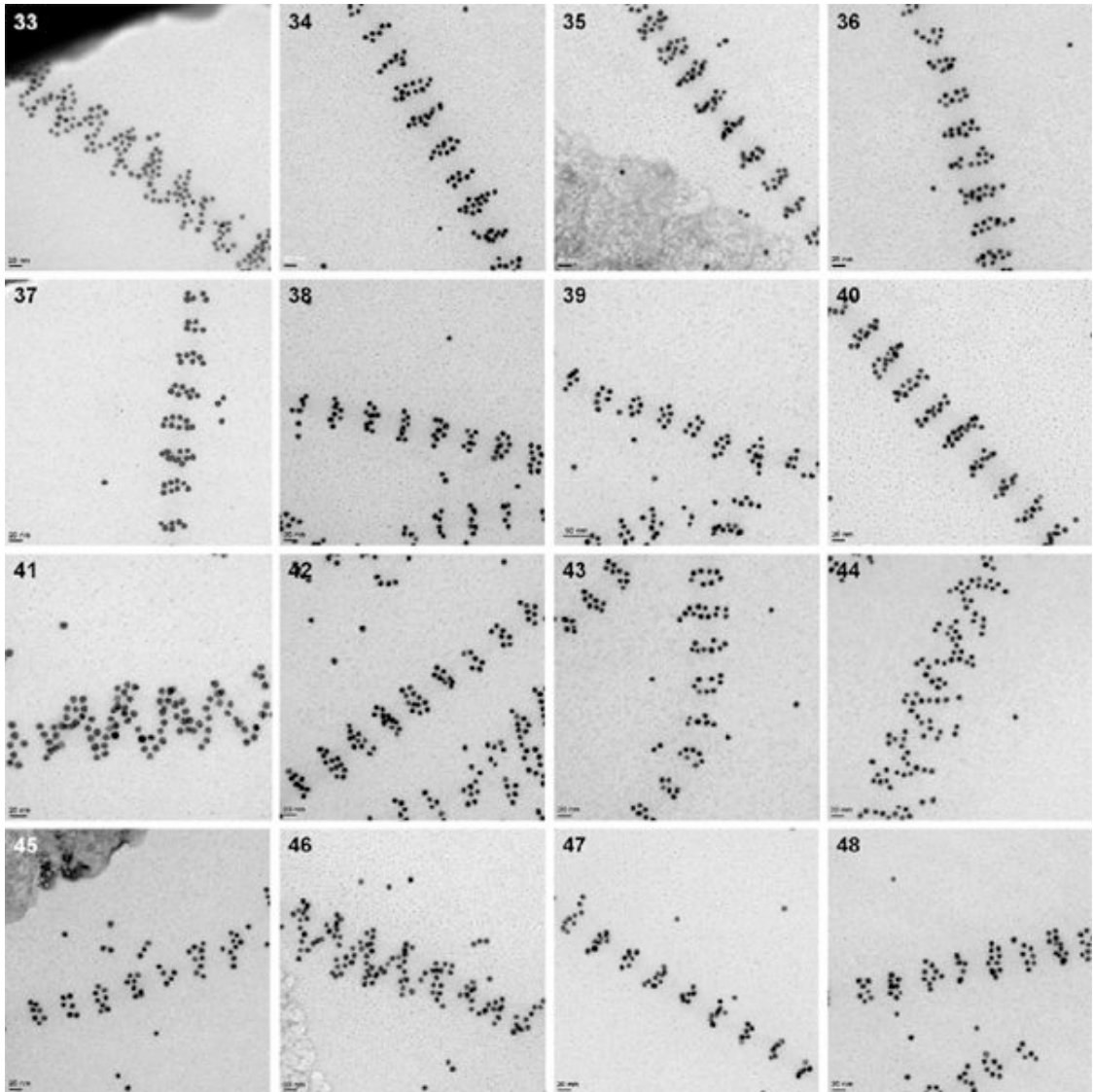
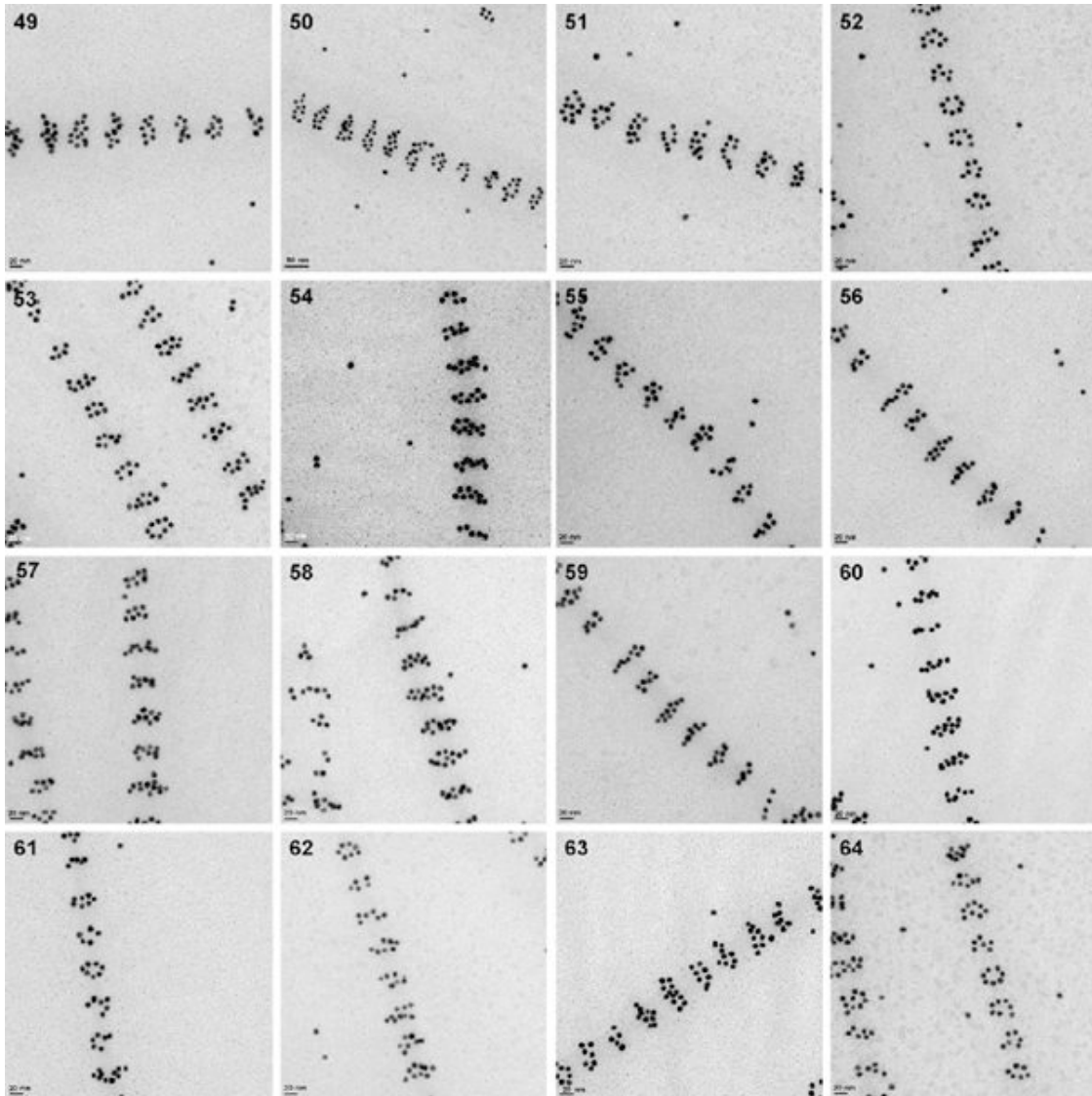


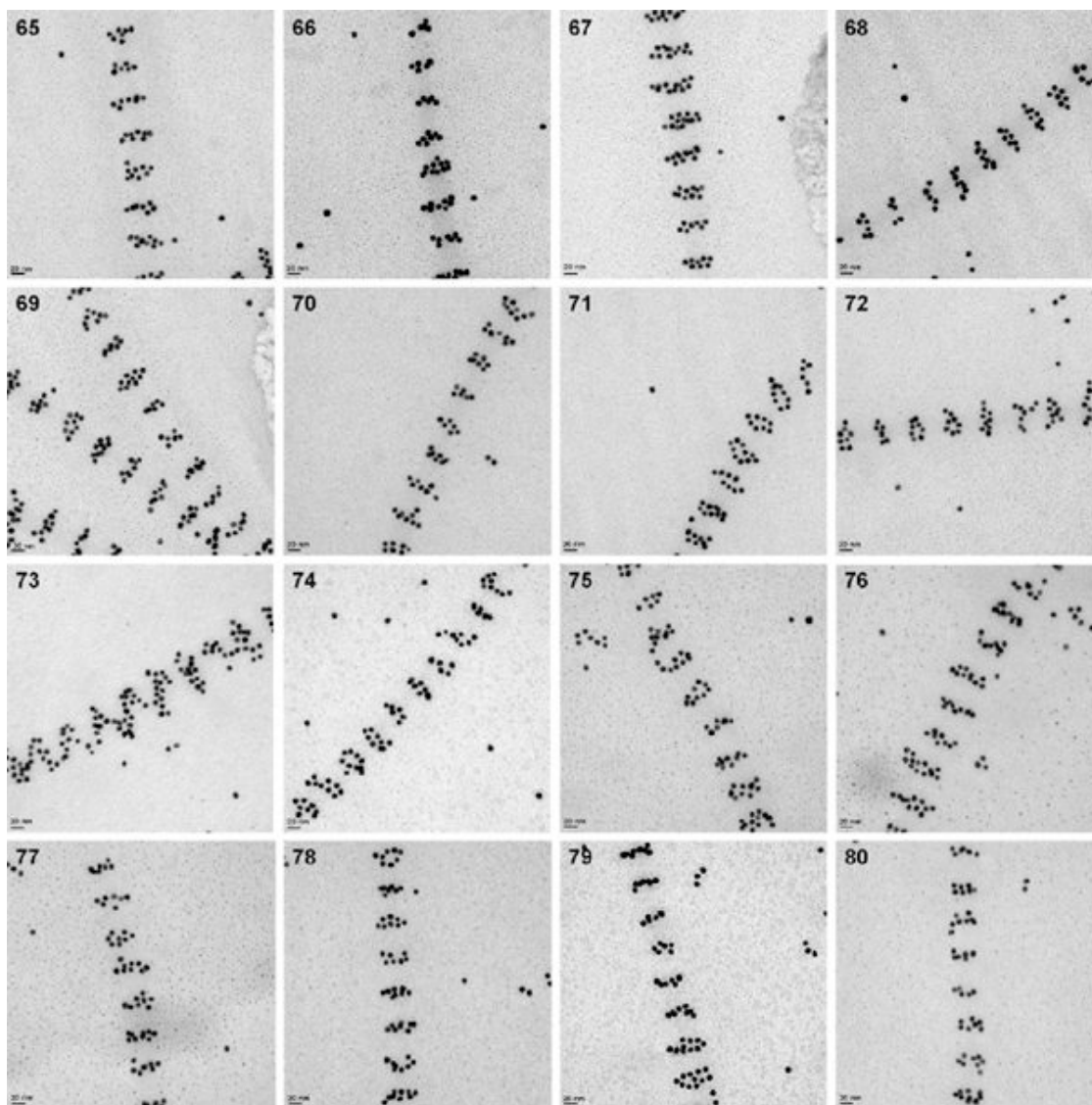
Figure S7. Additional zoom-in TEM images of DNA tubes with 10 nm AuNps in the A-tile.











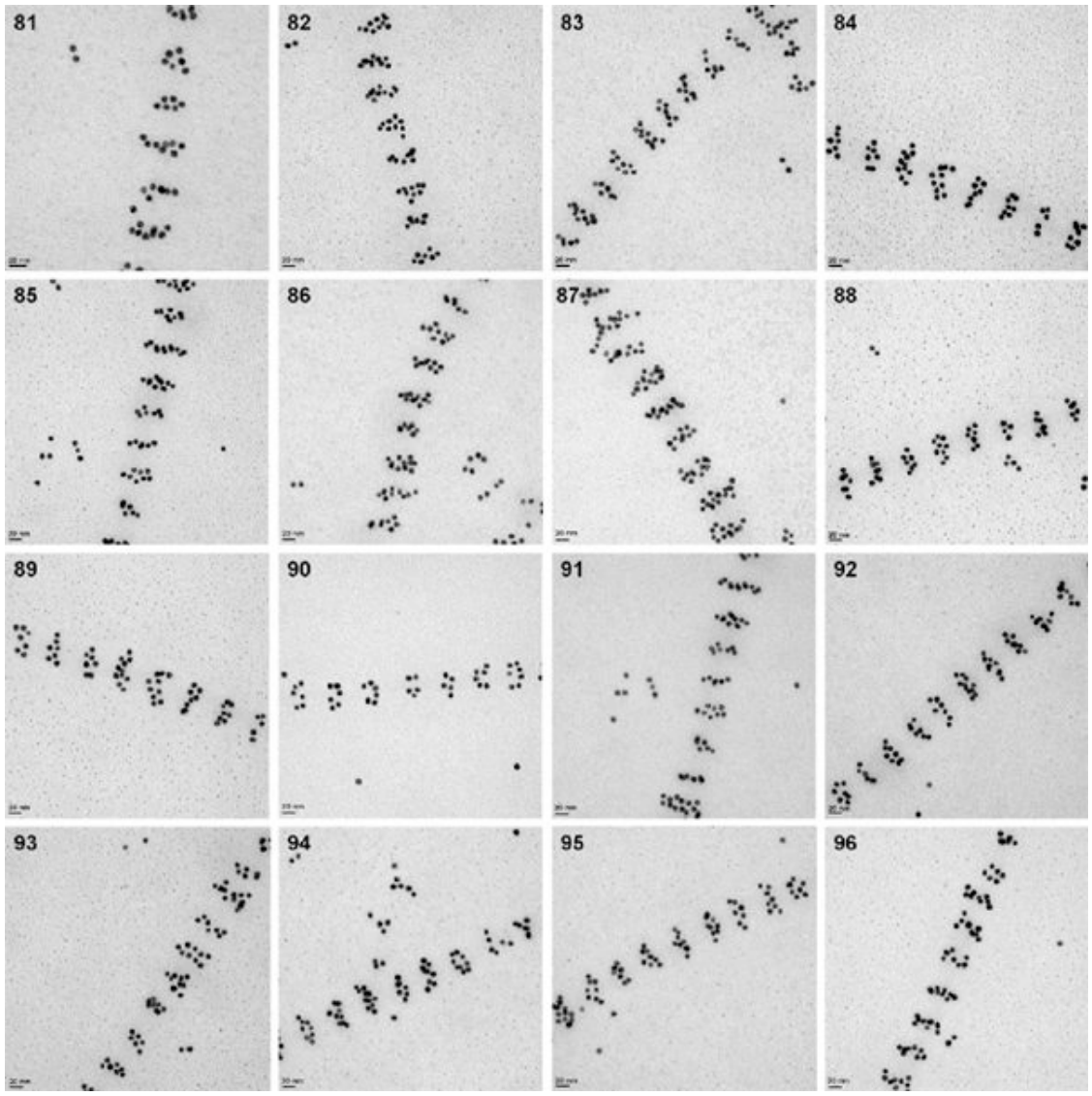
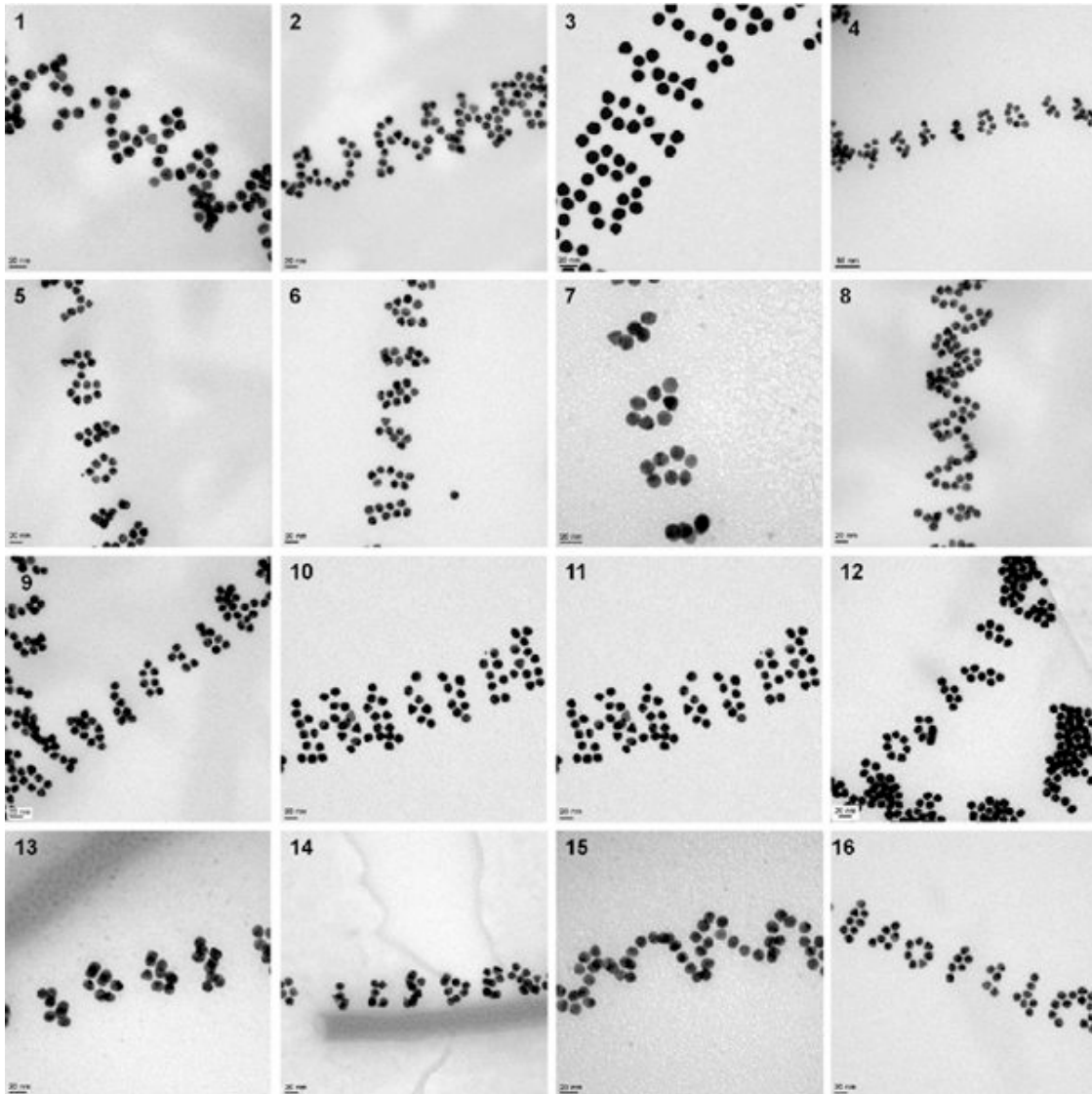
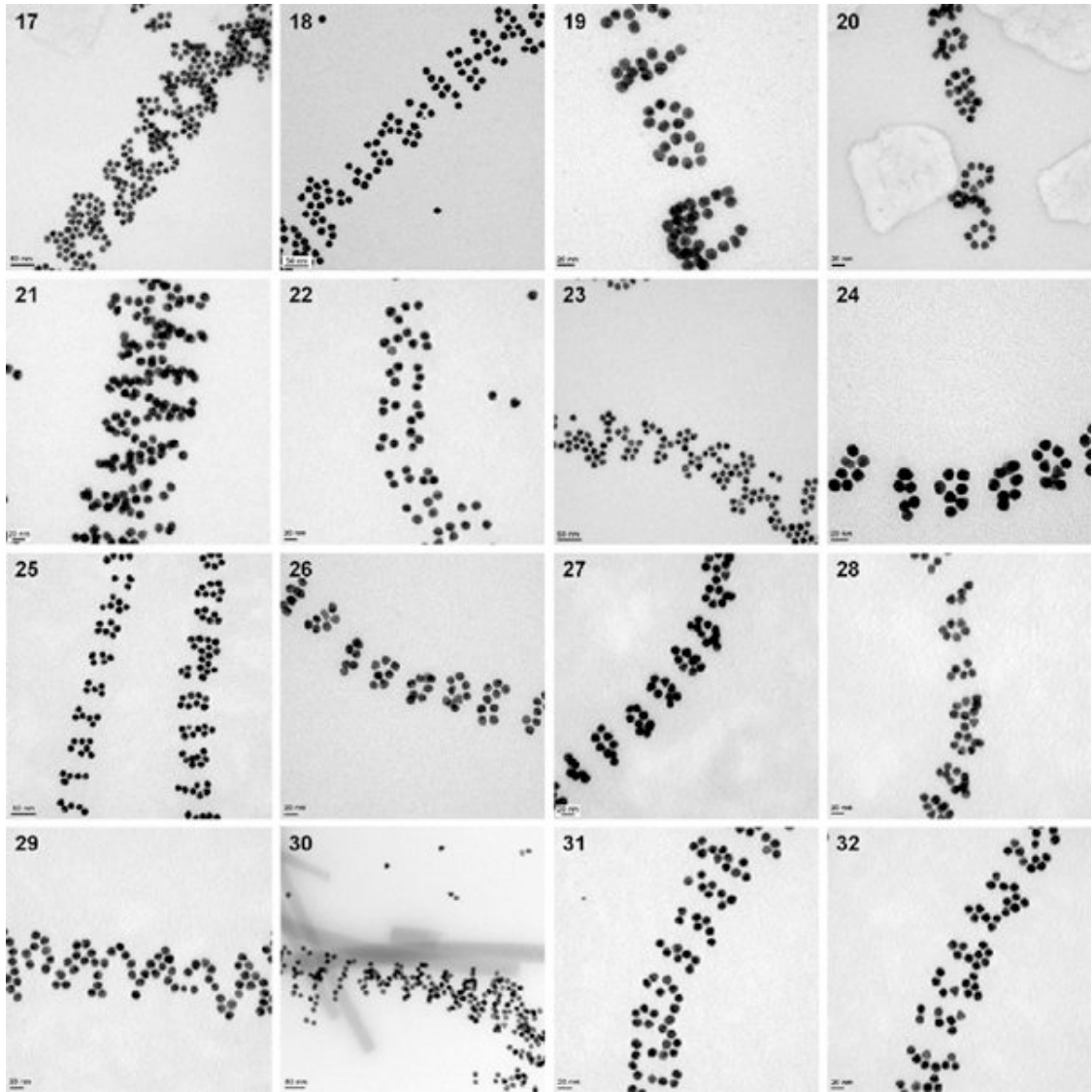
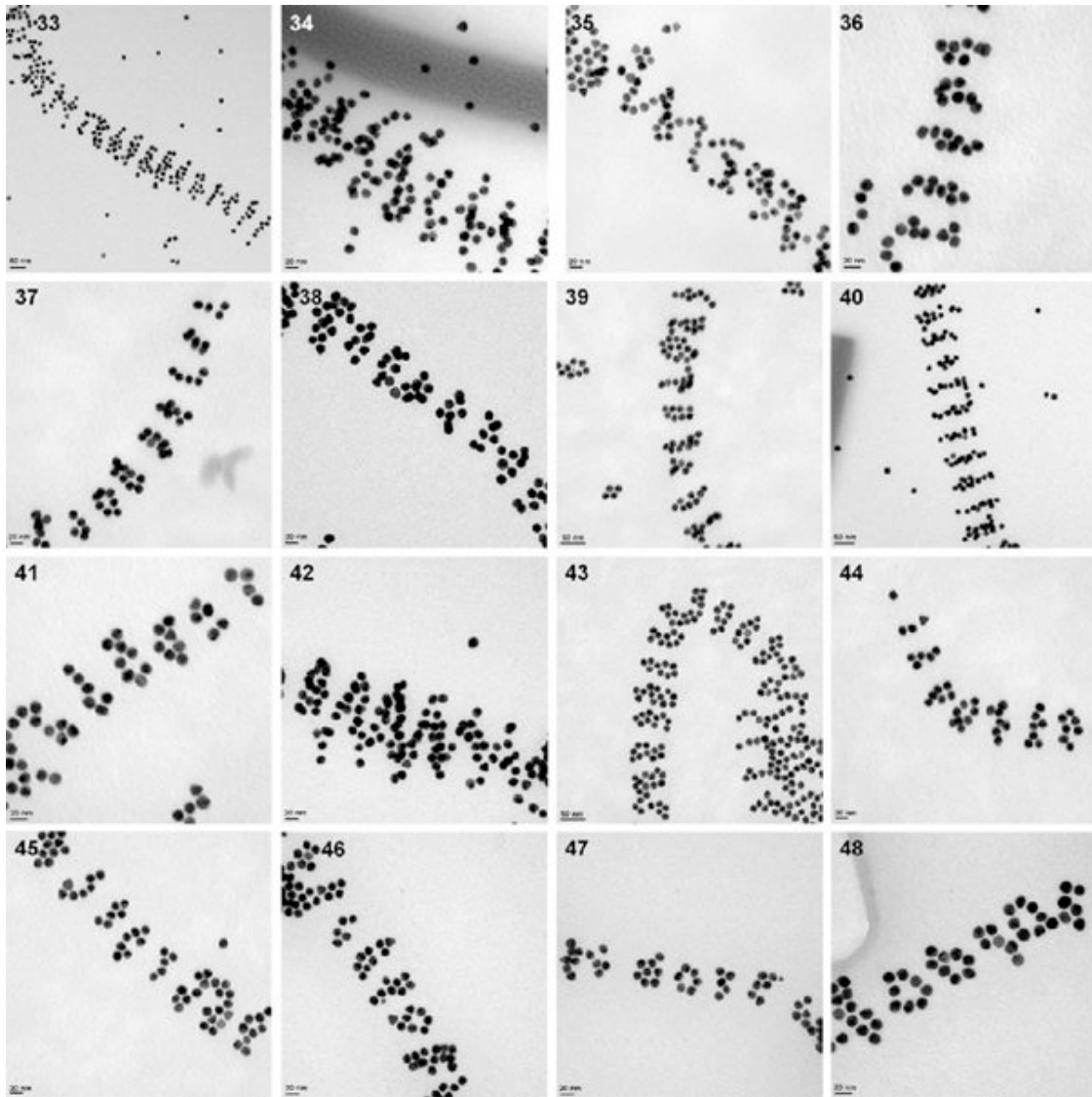
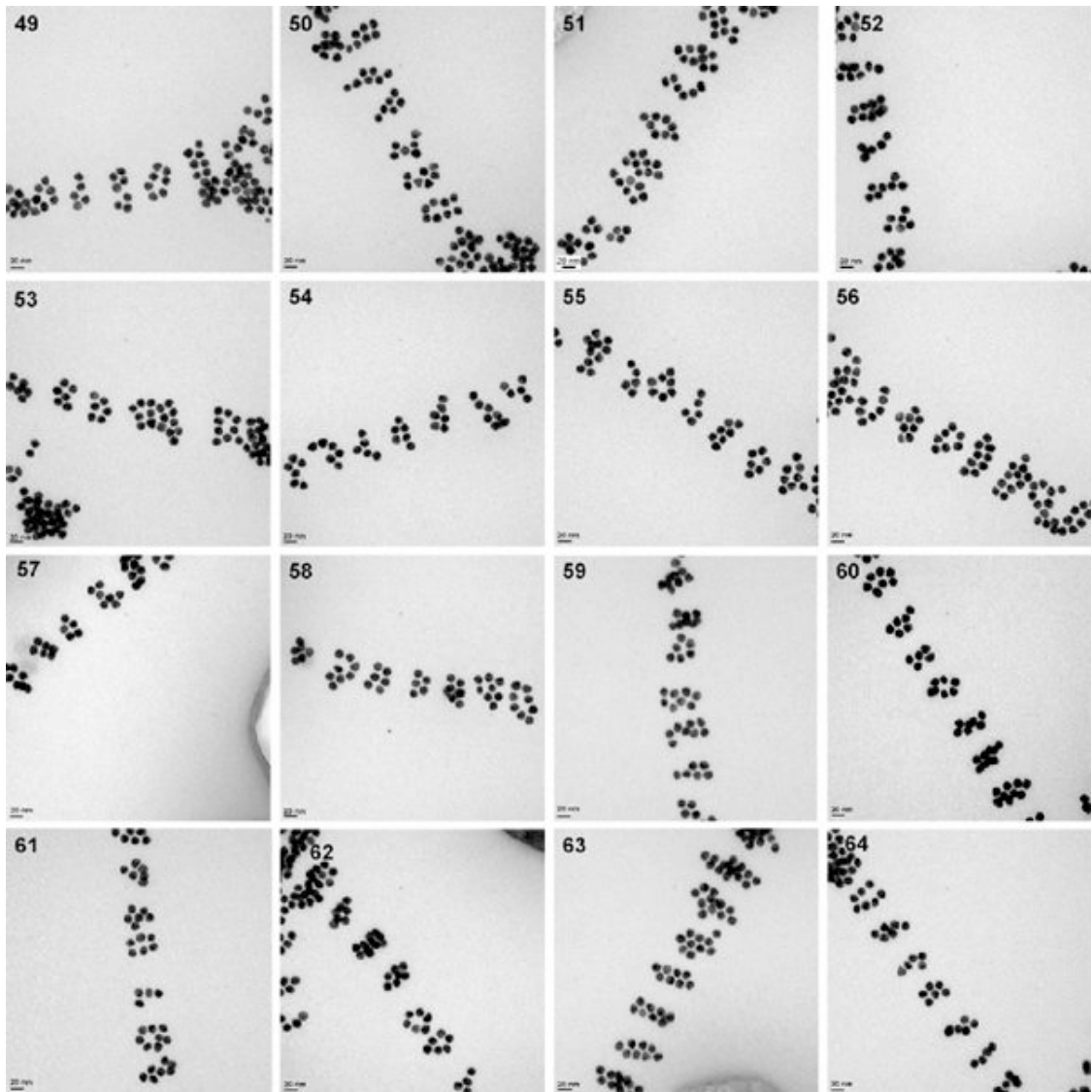


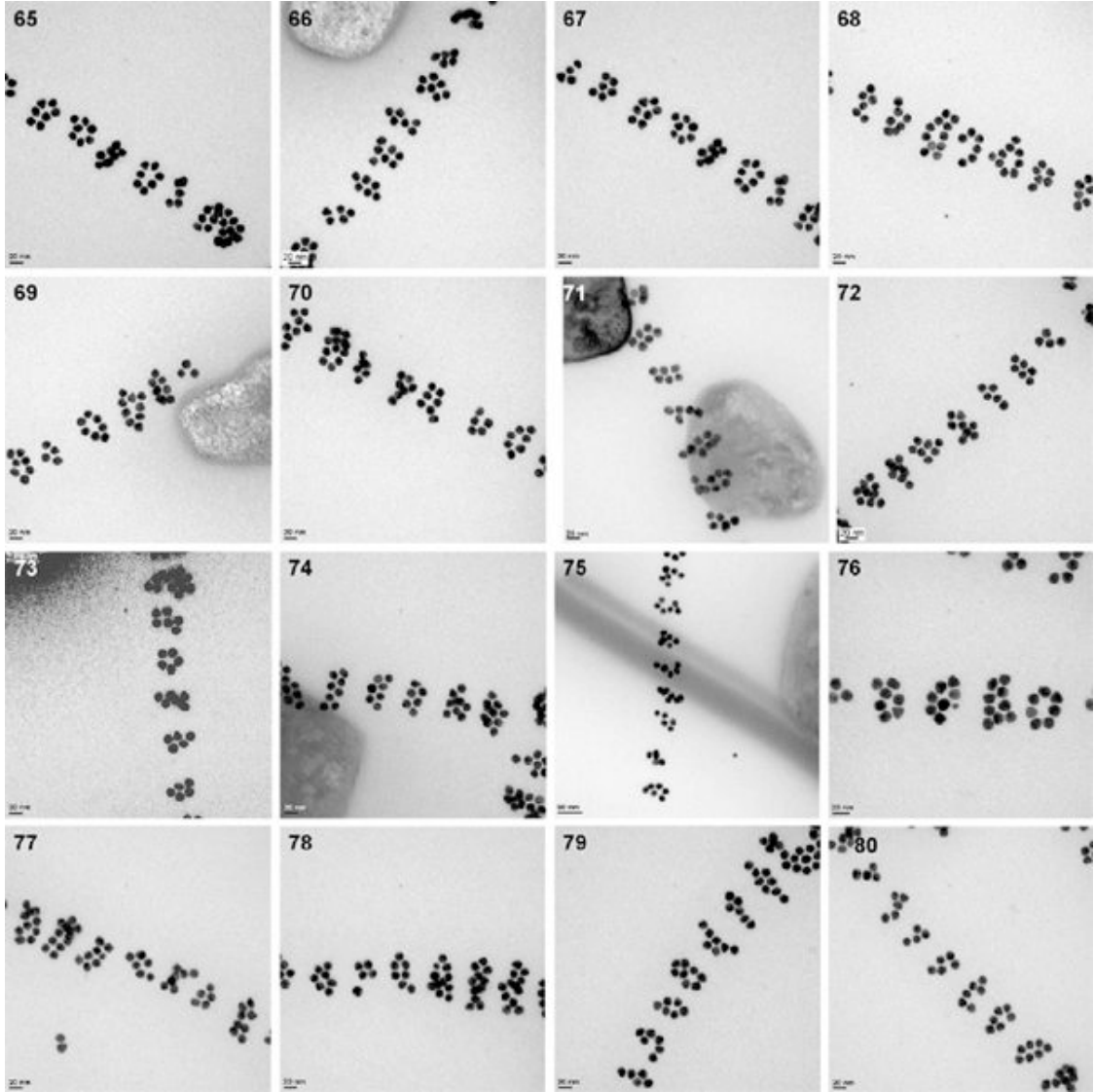
Figure S8. Additional zoom-in images of DNA tubes with 15 nm AuNps in the A-tile.











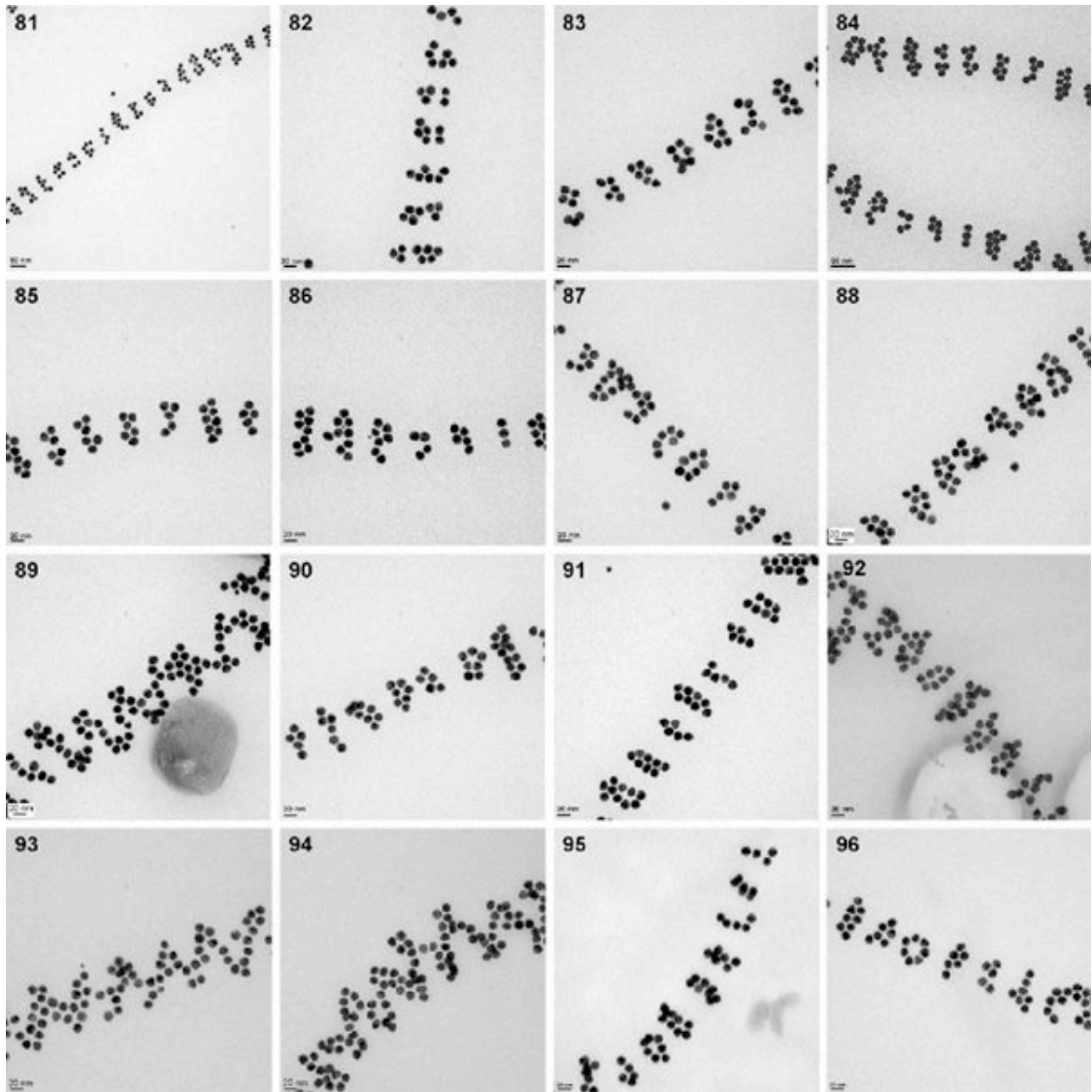


Figure S9. Cryo-EM images of DNA tubes imaged at different title angles. DNA tubes are decorated with 10 nm AuNps. DNA tubes are showing splitting of a single spiral tube into two stacked ring tubes.

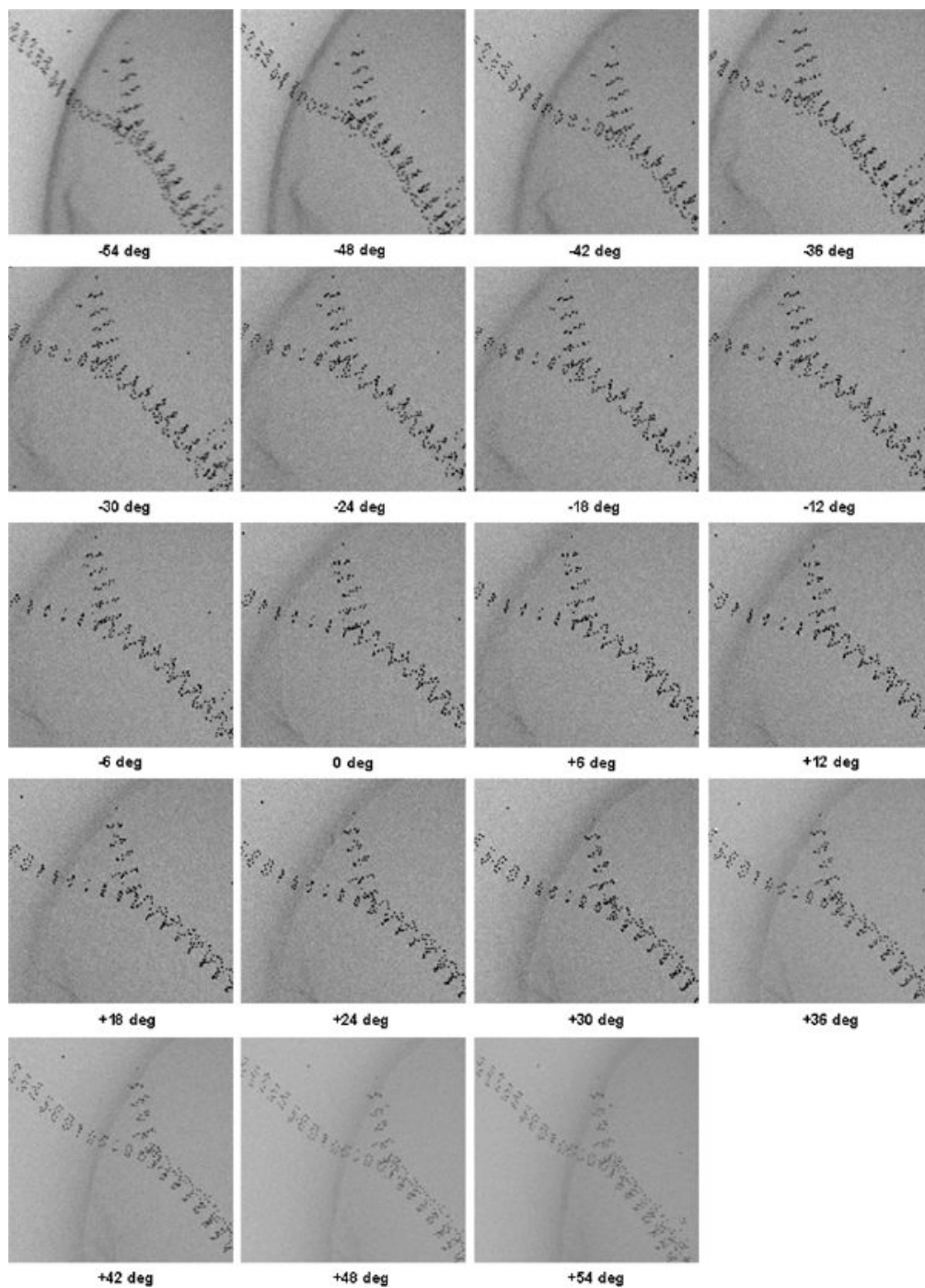


Figure S10. Cryo-EM images of stacked ring DNA tubes imaged at different title angles. The DNA tubes have A-tiles functionalized with 10 nm AuNps. Note the appearance of the circles of particles when tilt angles changed.

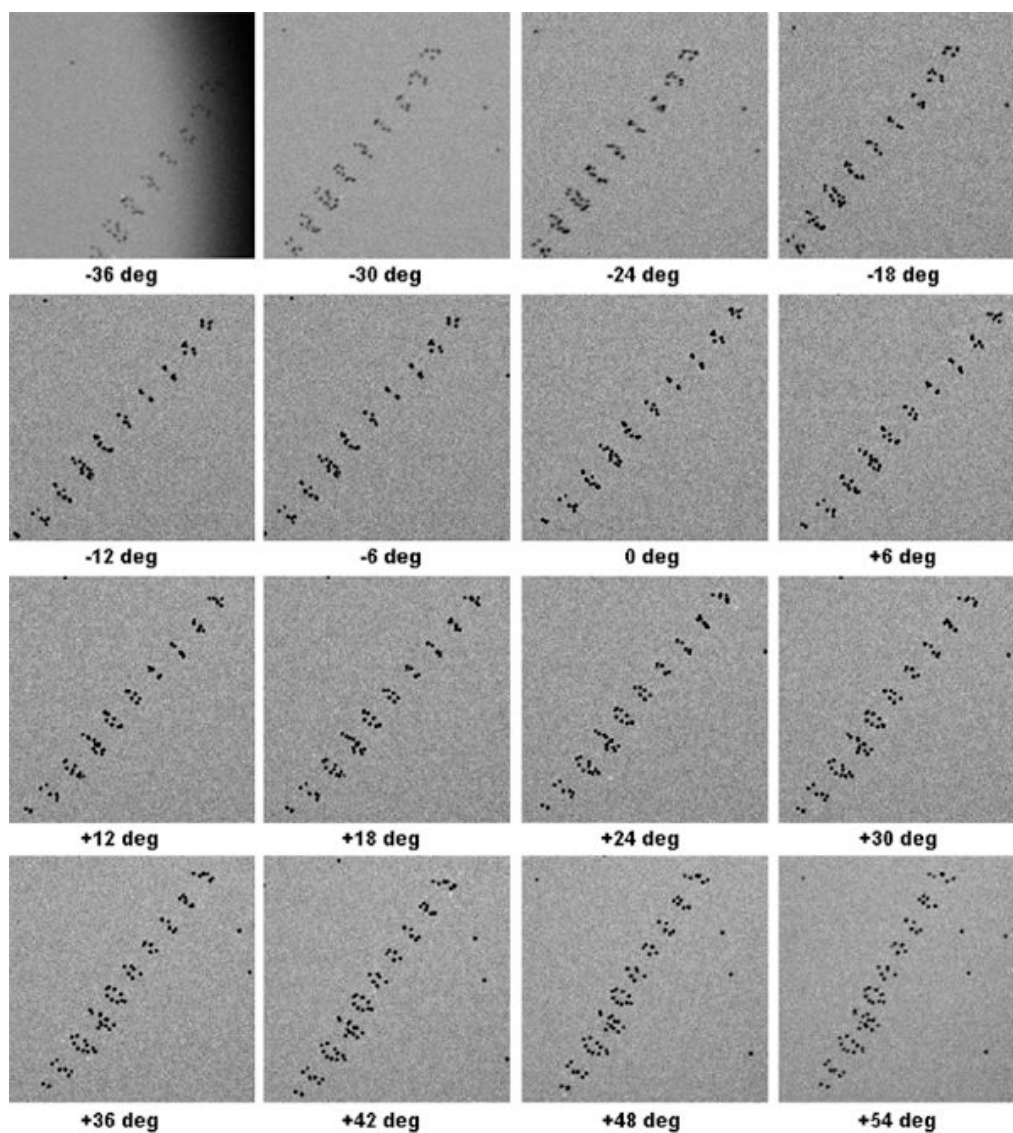


Figure S11. Cryo-EM images of 5 nm DNA tubes imaged at different tilt angles. Two DNA tubes can be observed with both spiral and stacked ring pattern of 5 nm AuNps. Note the left-handed chirality of the single spiral tube.

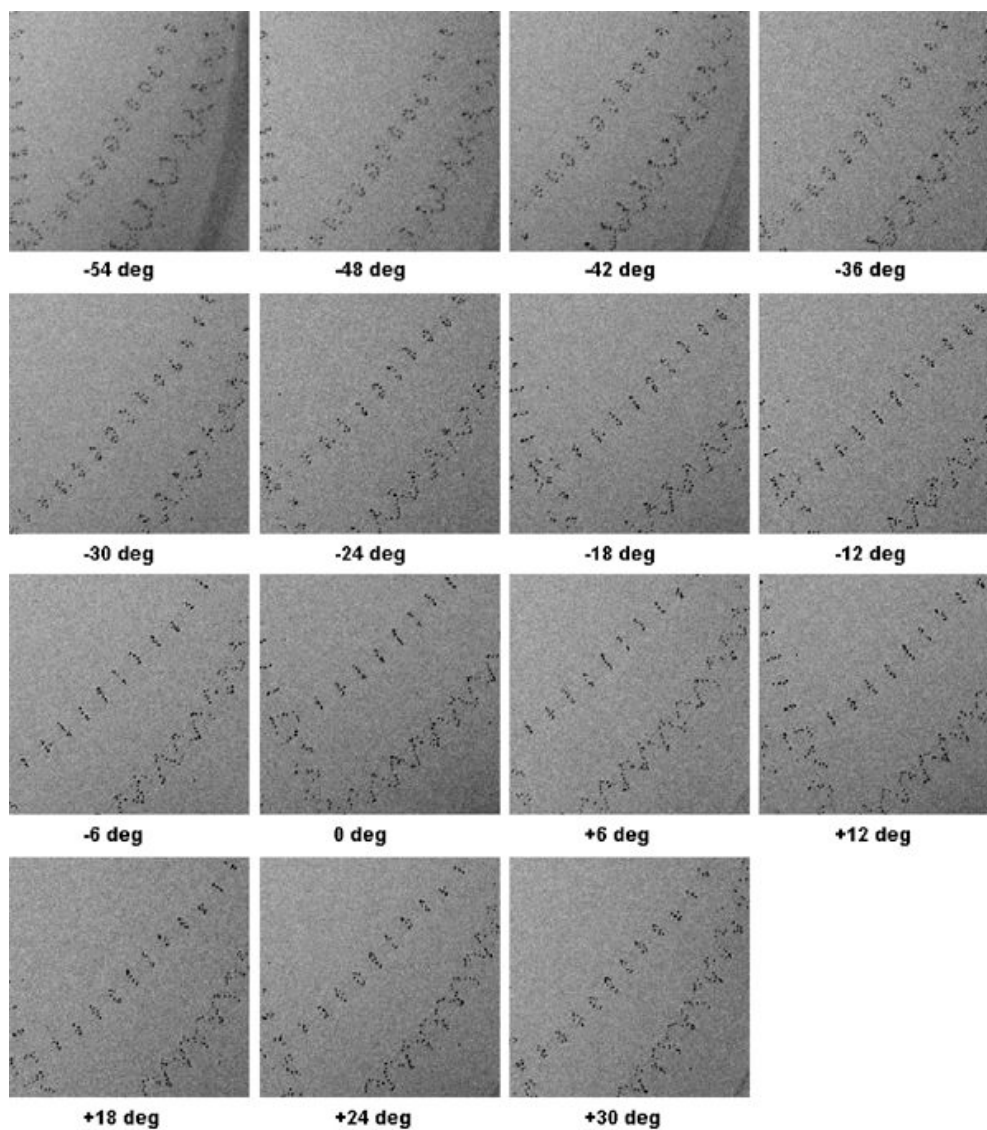


Figure S12. Cryo-EM images of a single spiral DNA tube with 5 nm AuNps imaged at different tilt angles. Note the left handed chirality of the single spiral tube.

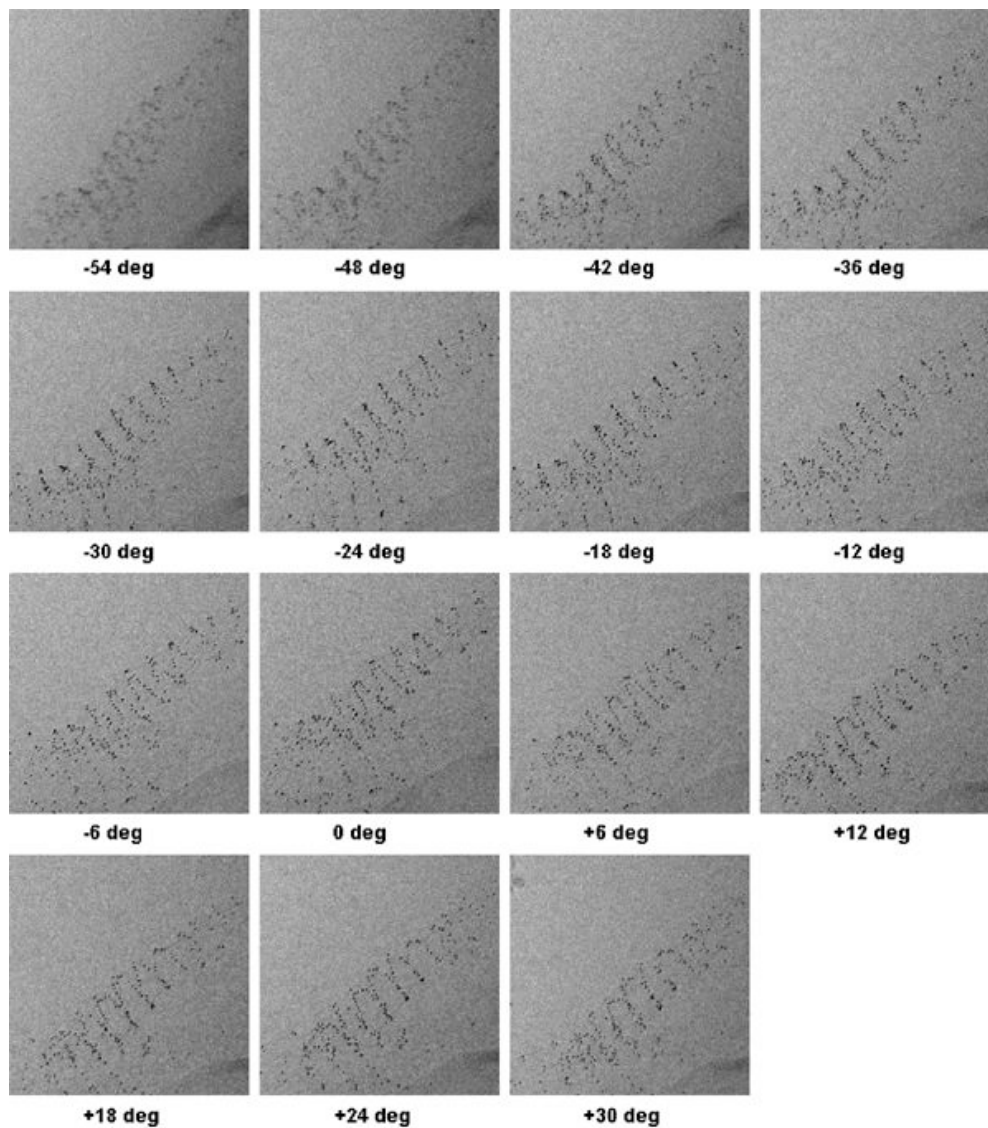


Figure S13. Cryo-EM images of a double spiral DNA tube with 5 nm AuNps and a random DNA loop on the opposite side imaged at different tilt angles.

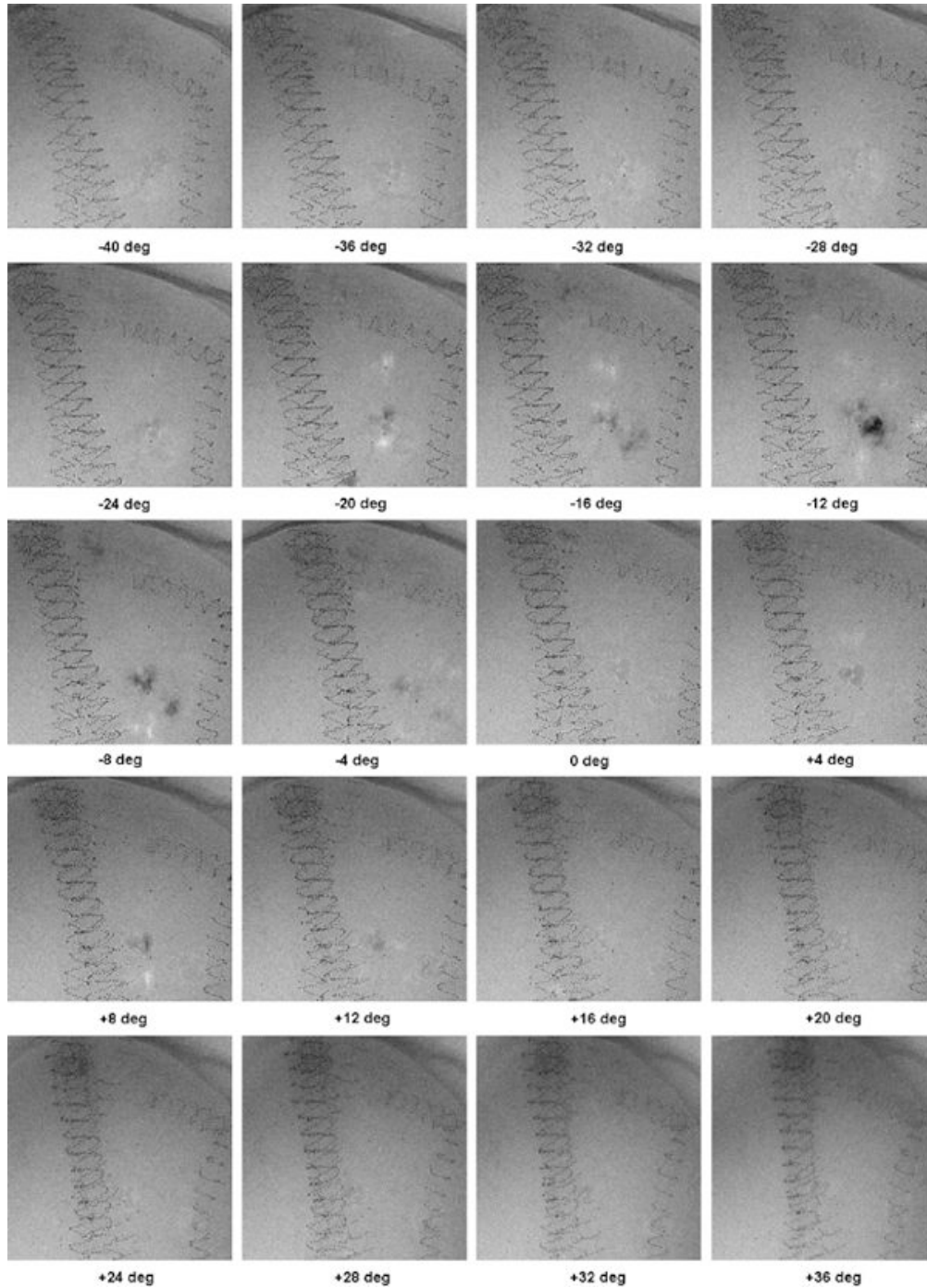
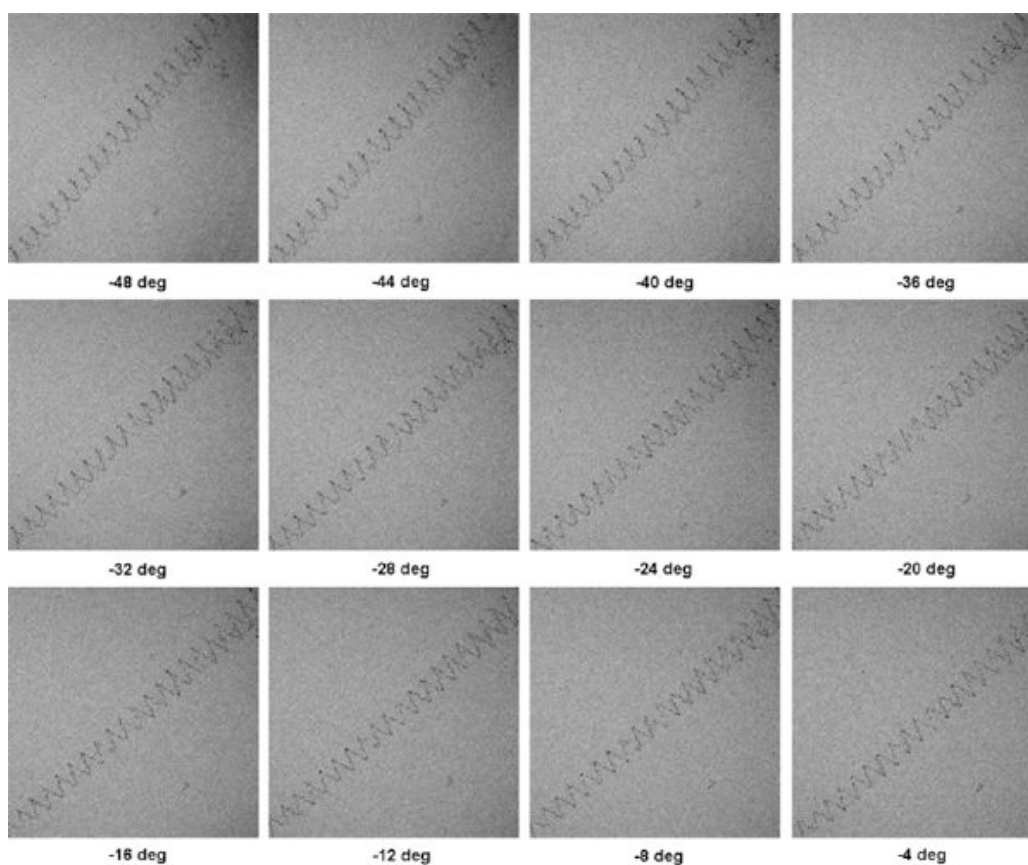
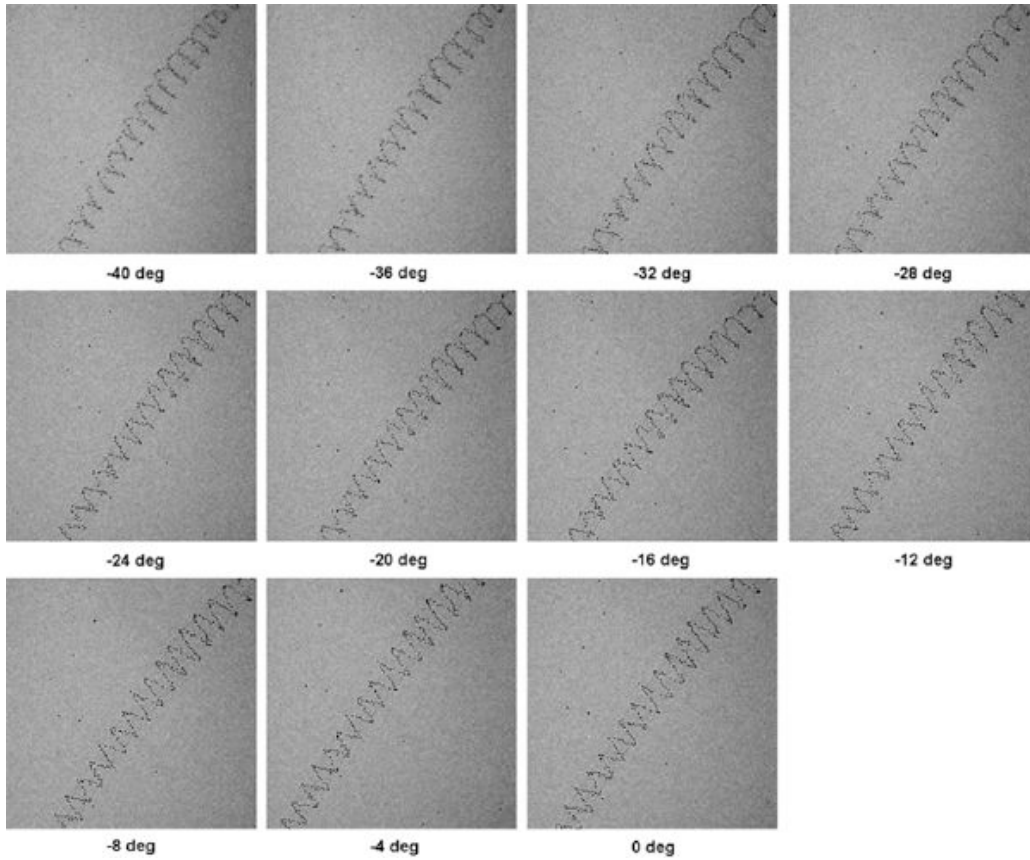


Figure S14. Additional examples of cryo-EM images of single spiral DNA tubes with 5 nm AuNps and a random DNA loop on the opposite side of the AuNps viewed at different tilt angles. Note the left-handed chirality of the tubes.

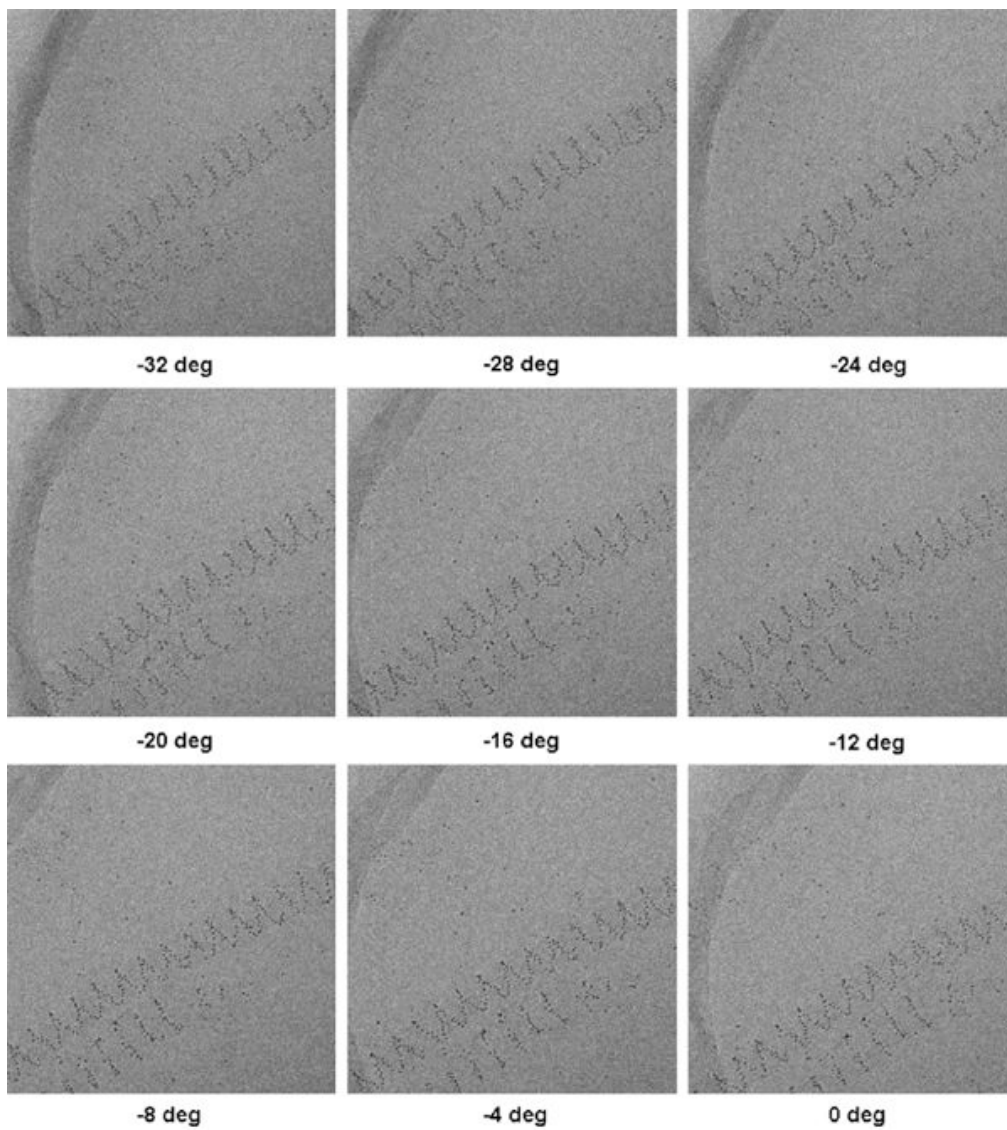
Example 1. Single spiral DNA tube



Example 2. Single spiral DNA tube



Example 3. Single spiral DNA tube



Example 4. Single spiral DNA tube

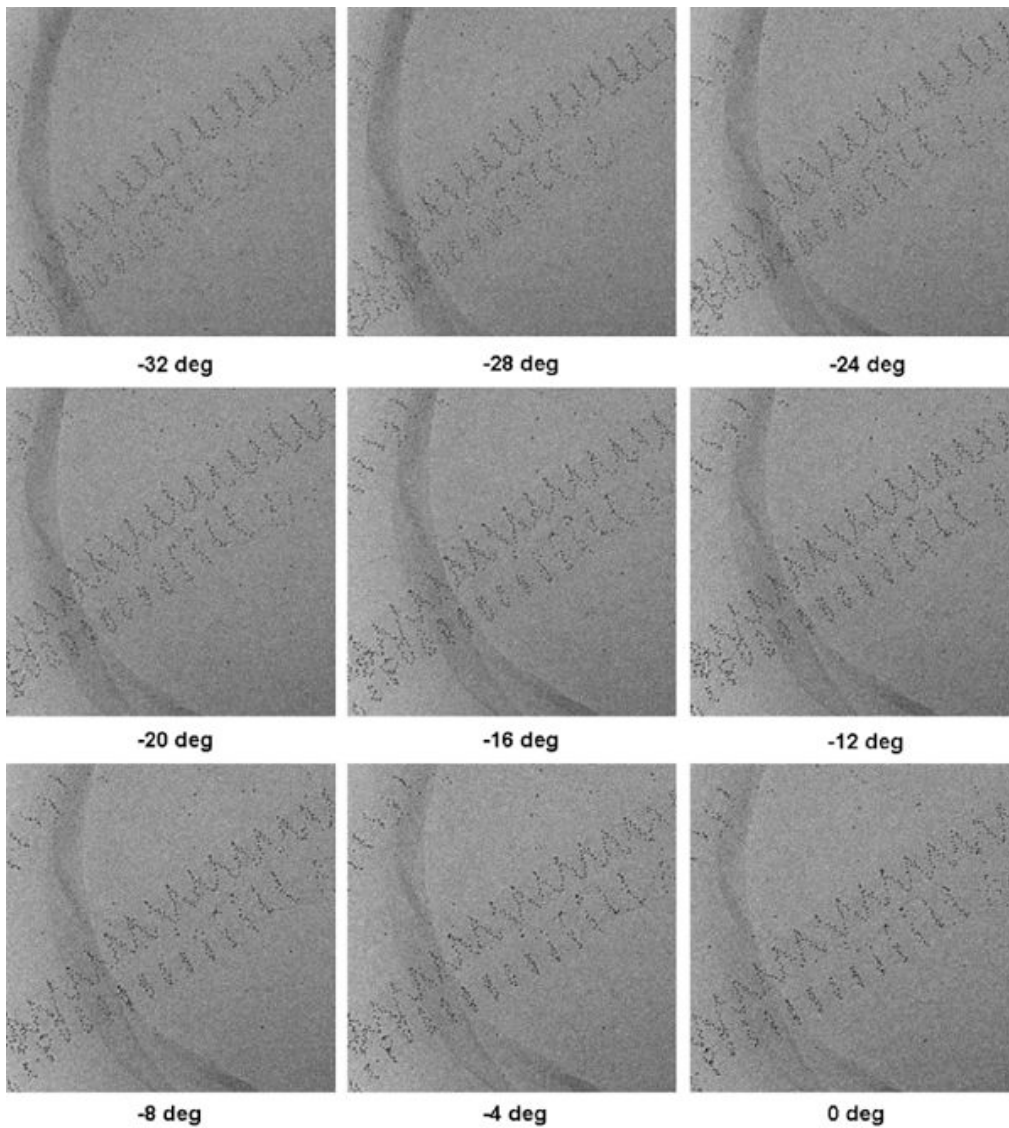


Figure S15. Some interesting features were observed in DNA tubes with 5 nm AuNps and a random DNA loop on the opposite face. A smooth conformational transition was imaged from single spiral to stacked ringed DNA tube and vice versa.

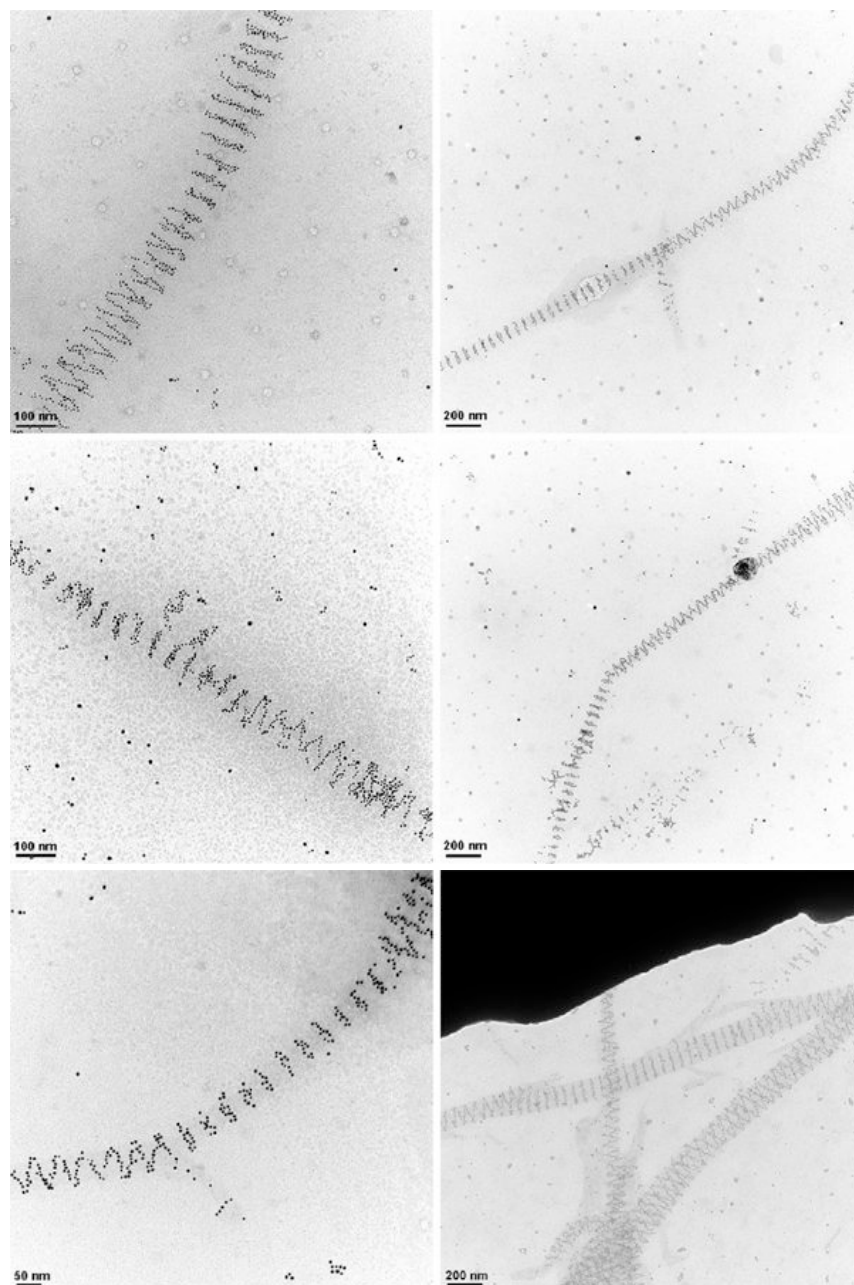
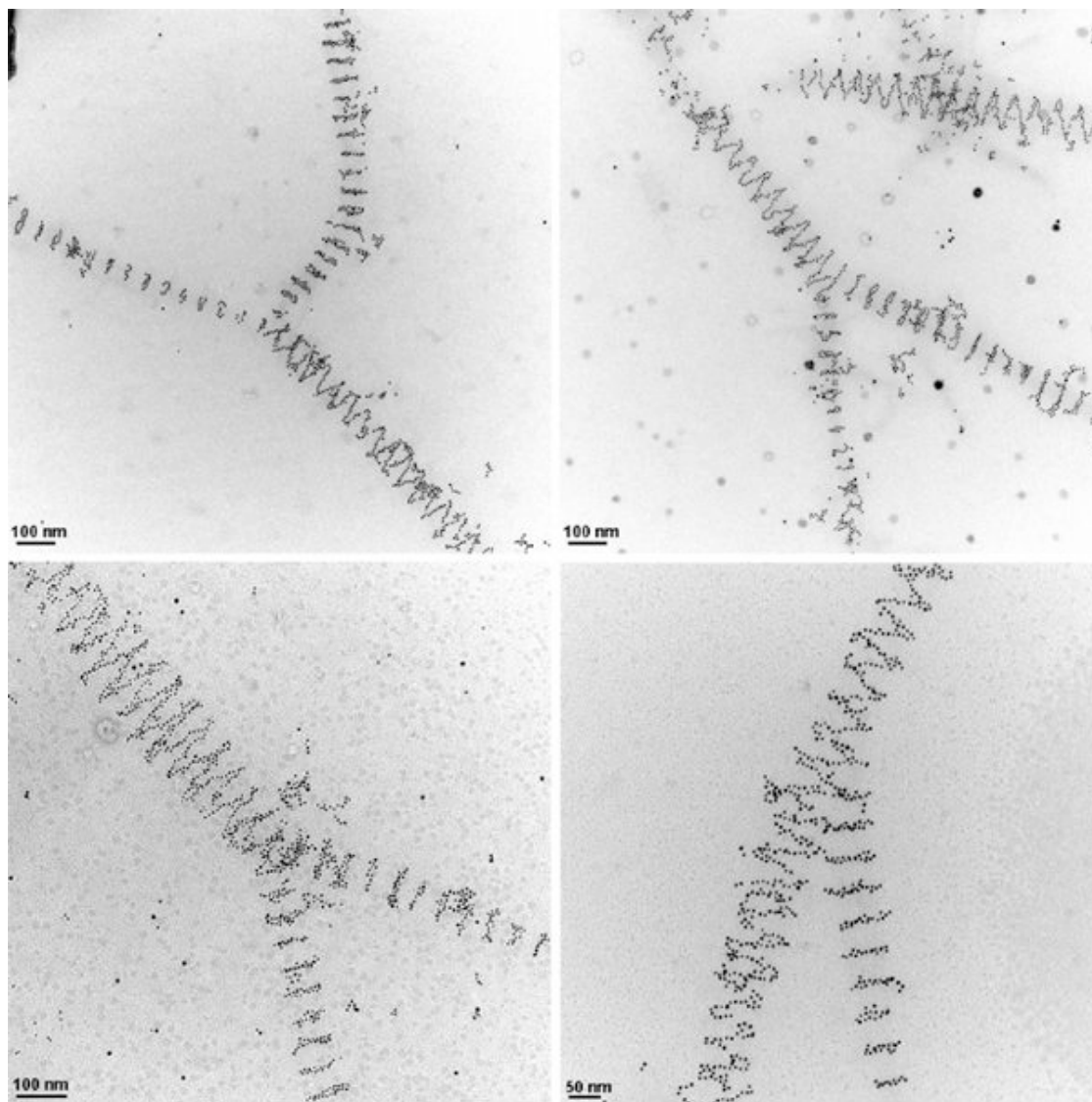


Figure S16. Splitting of single spiral DNA tubes into either two stacked ringed DNA tubes or one stacked-ringed and one spiral DNA tube was also observed during TEM analysis in DNA tubes consisting 5 nm AuNps and a random DNA loop on the opposite face.



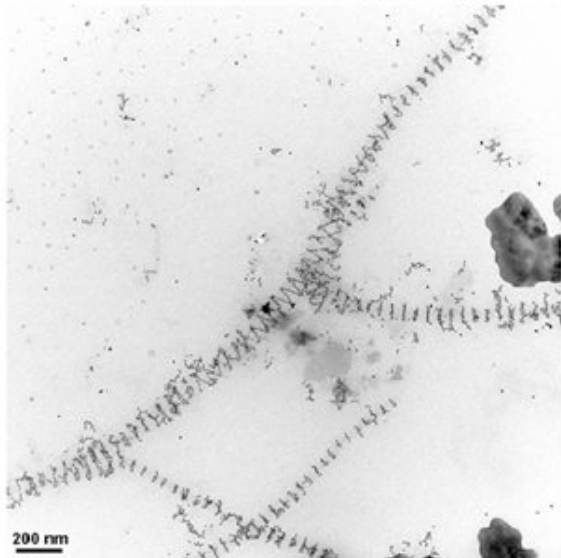
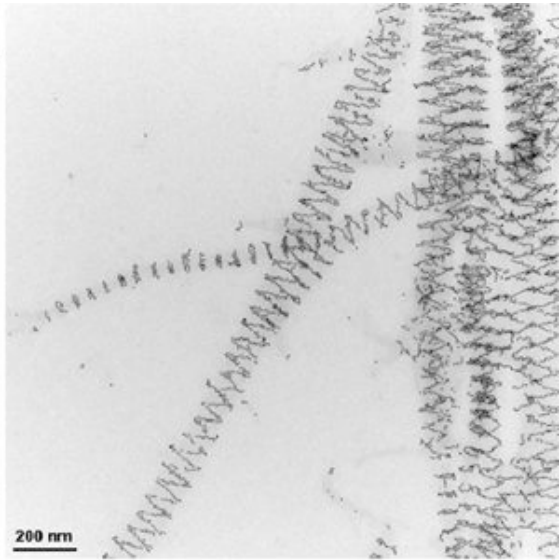
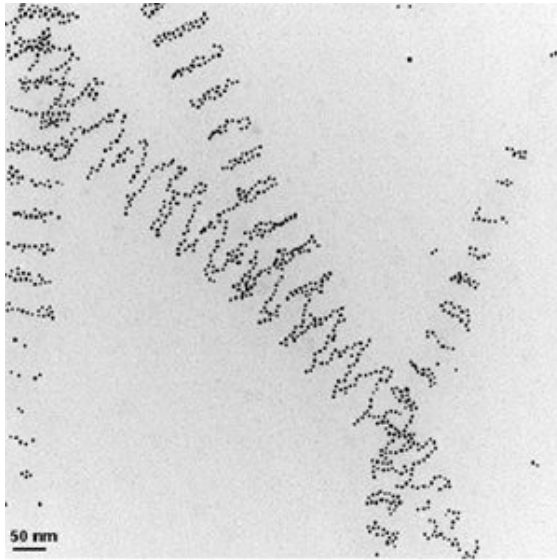
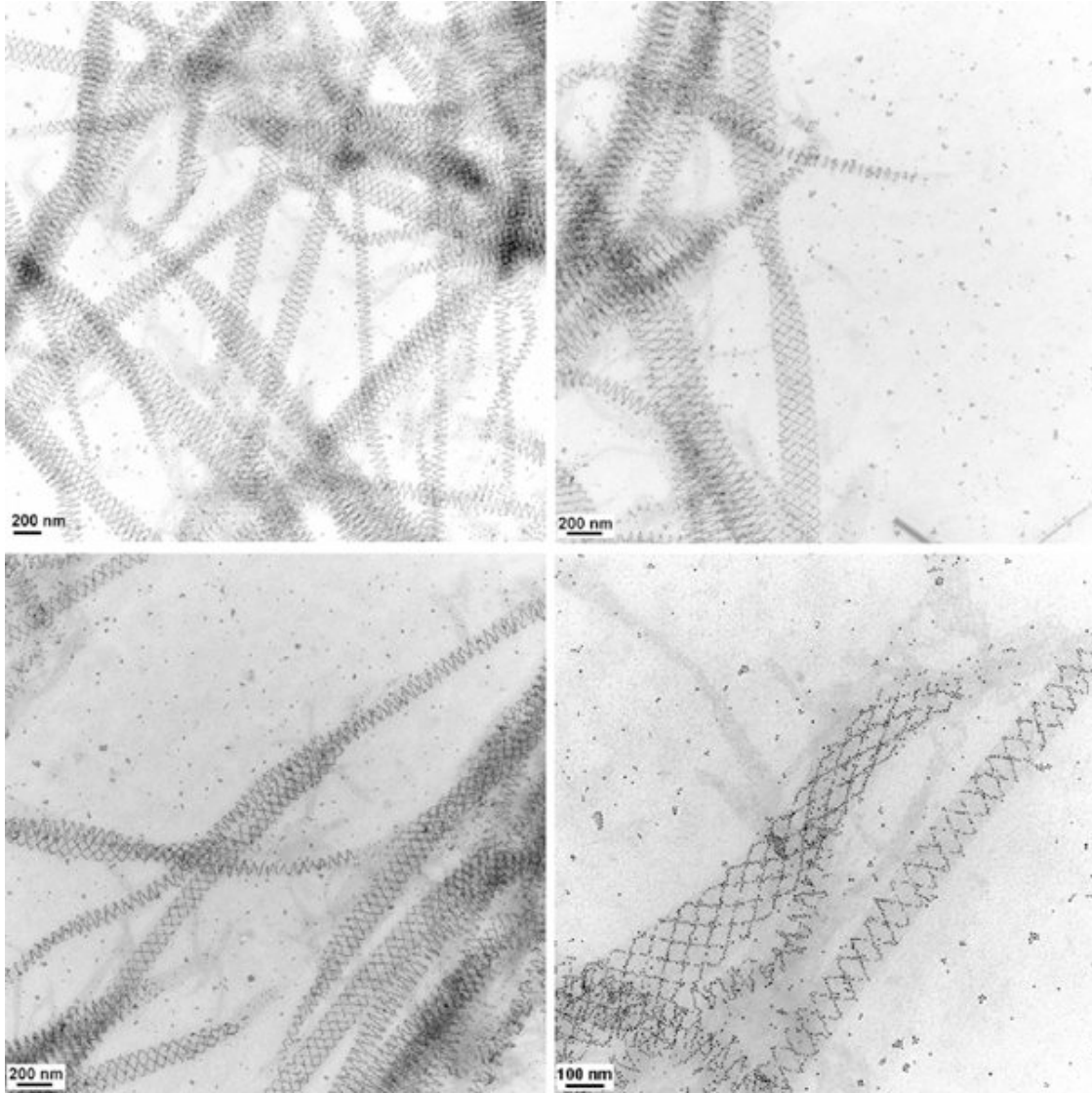
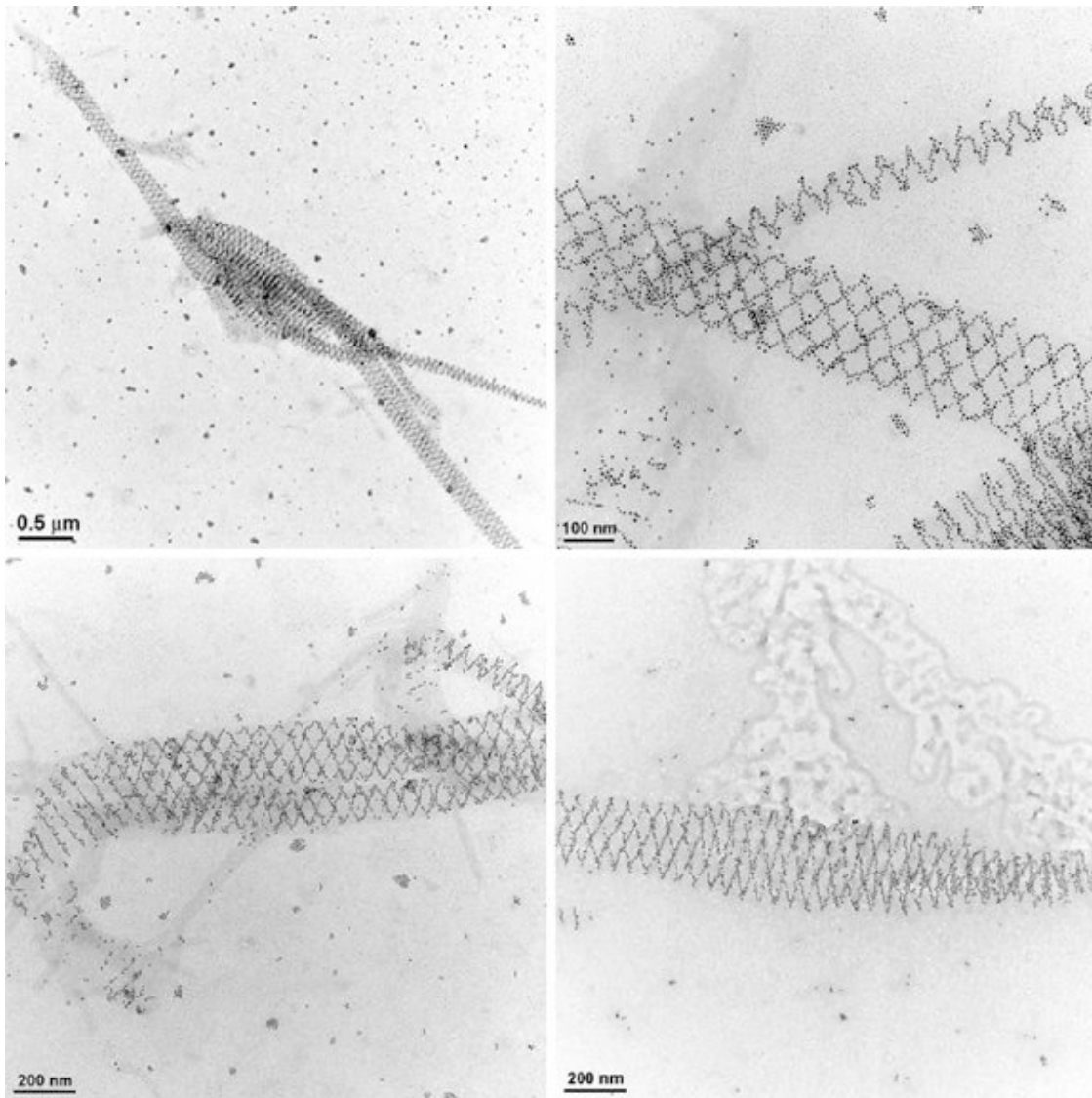


Figure S17. At higher concentrations of the constituent DNA elements (300 nM), spiral tubes with mixed conformations were observed in the TEM analysis of the sample with 5 nm AuNps and a random DNA loop facing the opposite sides. Spiral DNA tubes ranging from single spiral to double spiral and nested spirals were observed, which are presented below in a few representative TEM images (include zoom-outs and zoom-ins).





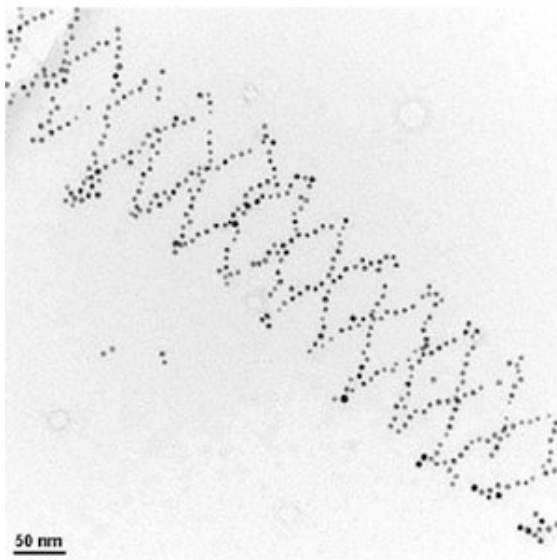
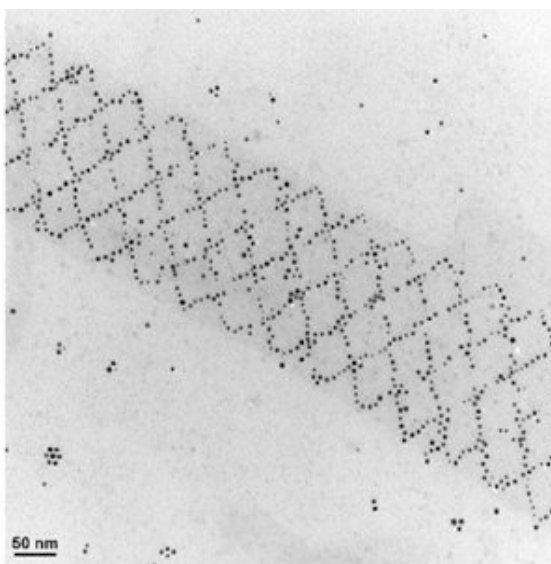
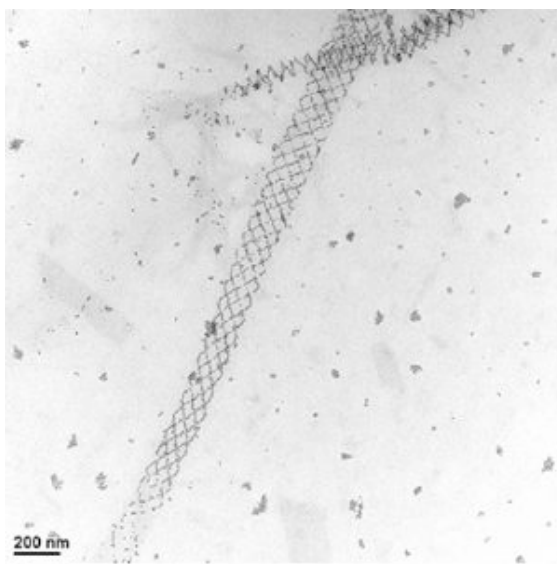


Figure S18. Additional zoom-in TEM images of the DNA tubes with both 5 nm and 10 nm AuNps on opposite faces. It can be seen from some images that the circumference width for the 5 nm particle tube is smaller than that of the 10 nm particle tube.

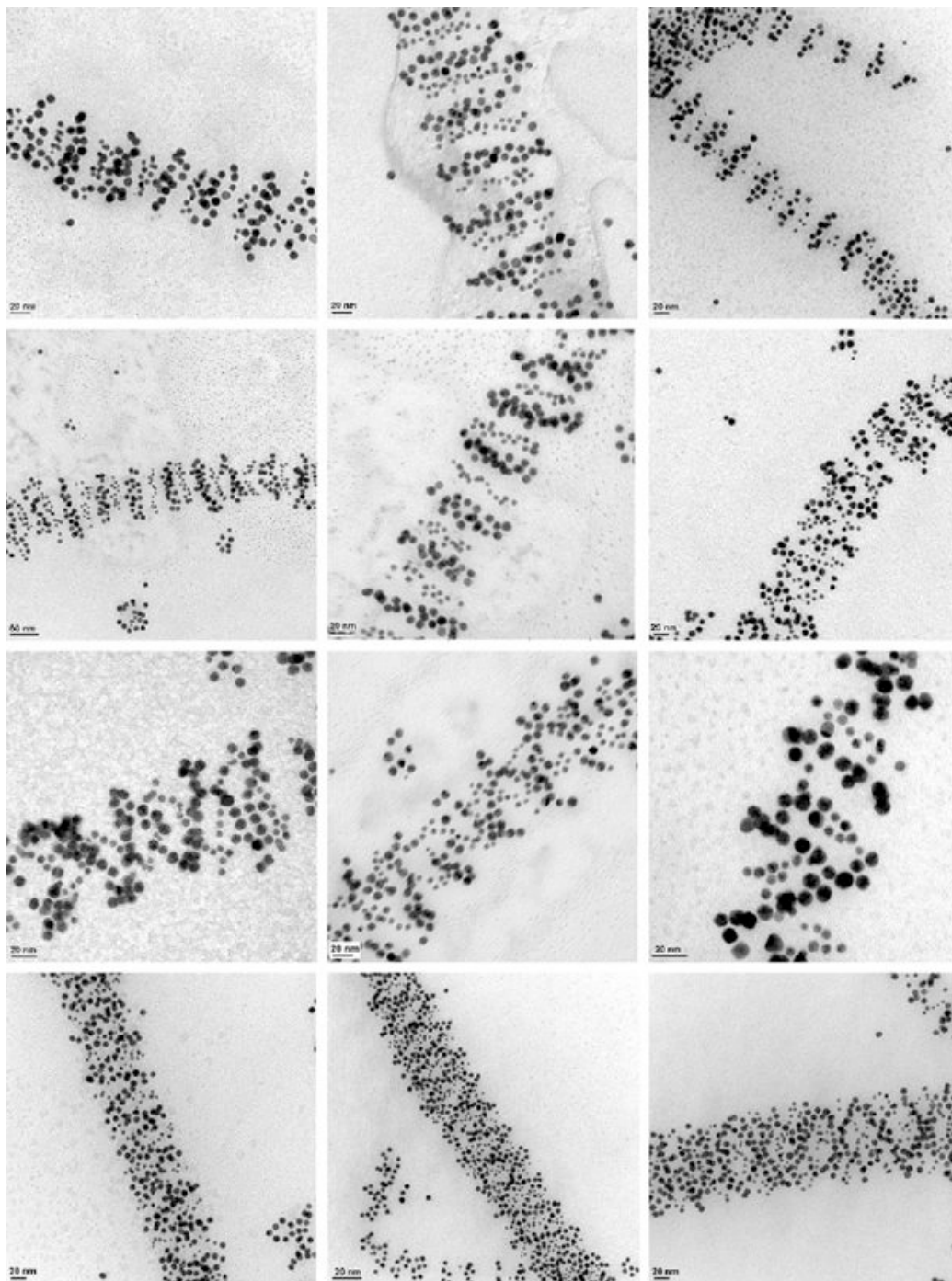
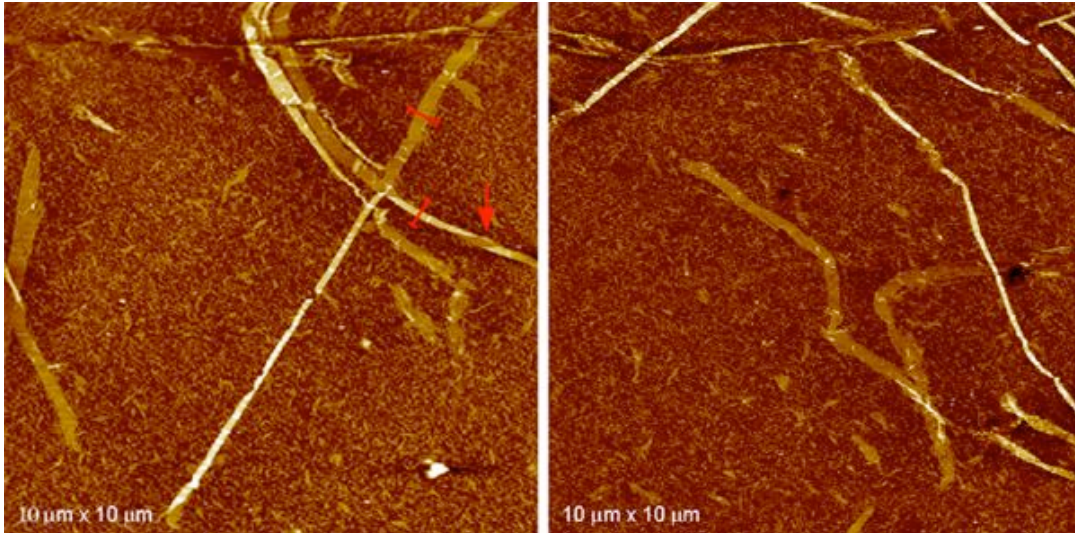
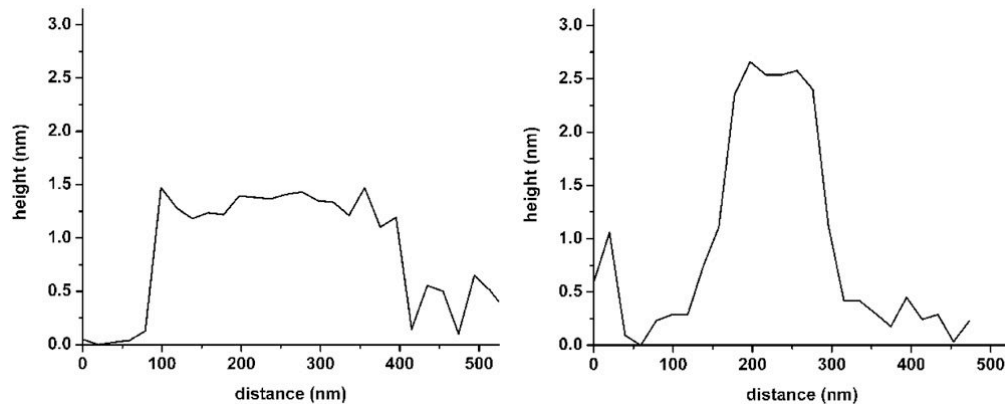


Figure S19. AFM images of the DX-DNA arrays. DX-DNA arrays were assembled using all of the constituent strands as shown in Figure S1. The sample mostly formed two-dimensional DNA arrays along with a few DNA tubes. Height profiles of the 2D arrays and DNA tubes are pointed out on the AFM image in the red-colored cross-bars. DNA tubes possessed an increased height of ~ 2.5 nm as compared to the ~ 1.4 nm thick single-layered 2D DNA arrays.



Height profiles of the 2D DNA arrays and DNA tube.



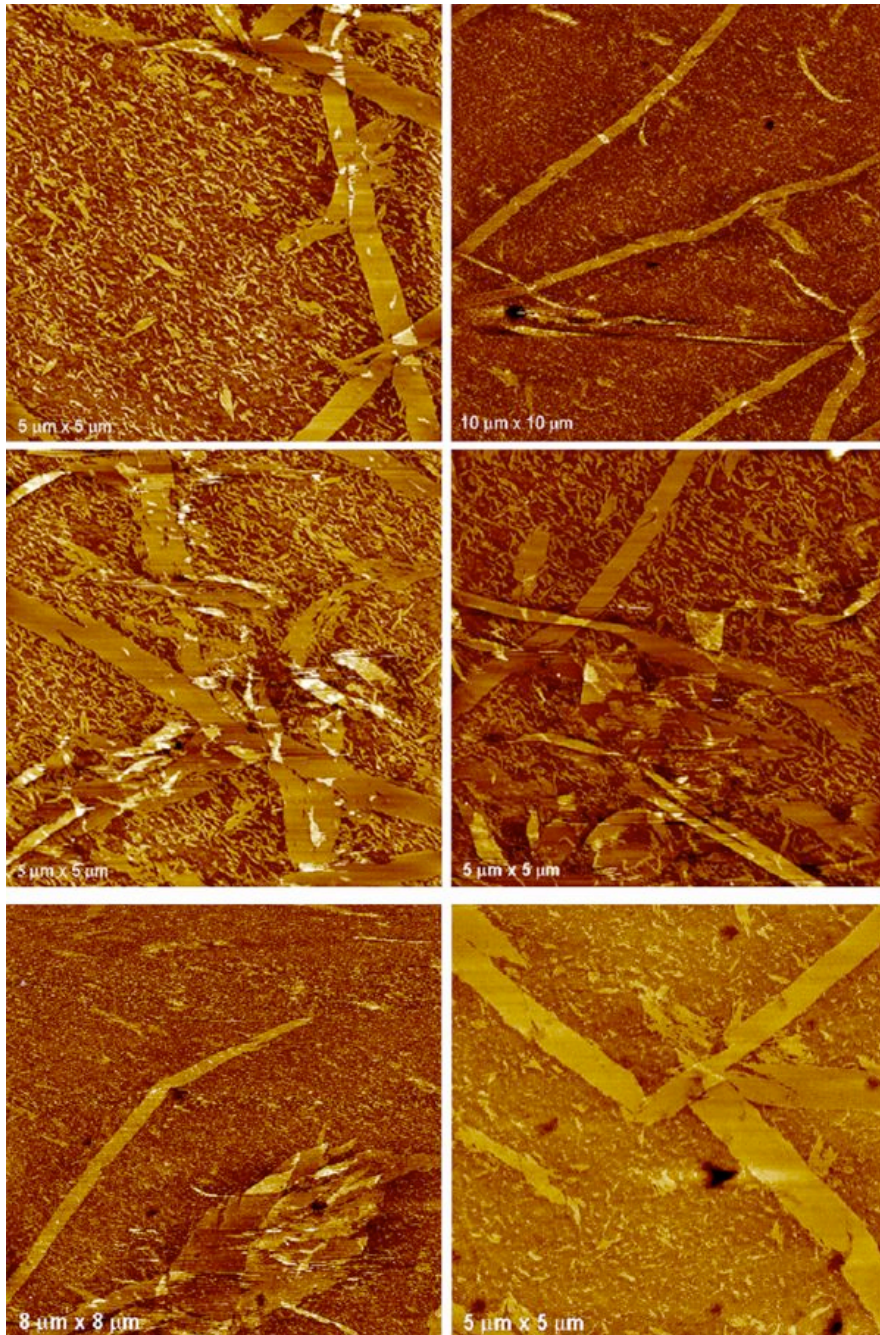


Figure S20. TEM images of DNA arrays wherein both DX-A and DX-C DNA tiles are modified with 5 nm AuNps. The doubly-modified sample showed both DNA tubes and 2D arrays.

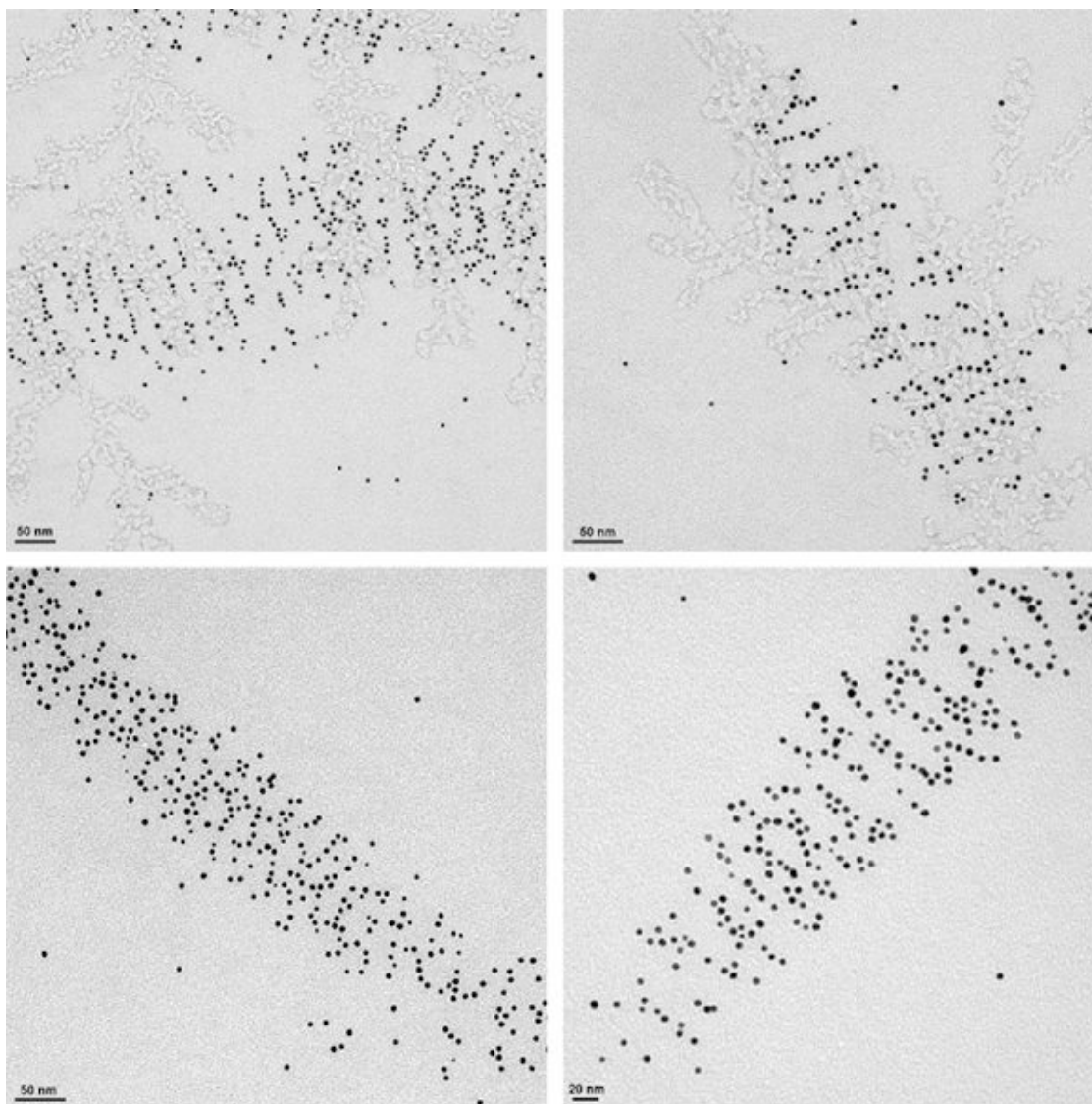


Figure S21. Representative TEM images of the DNA arrays where both DX-A and DX-C DNA tiles are modified with 10 nm AuNps. In contrast to the doubly-modified 5 nm AuNps DNA sample, the 10 nm AuNps sample formed only 2D arrays, presumably because of the significantly greater steric repulsions of the larger sized AuNps.

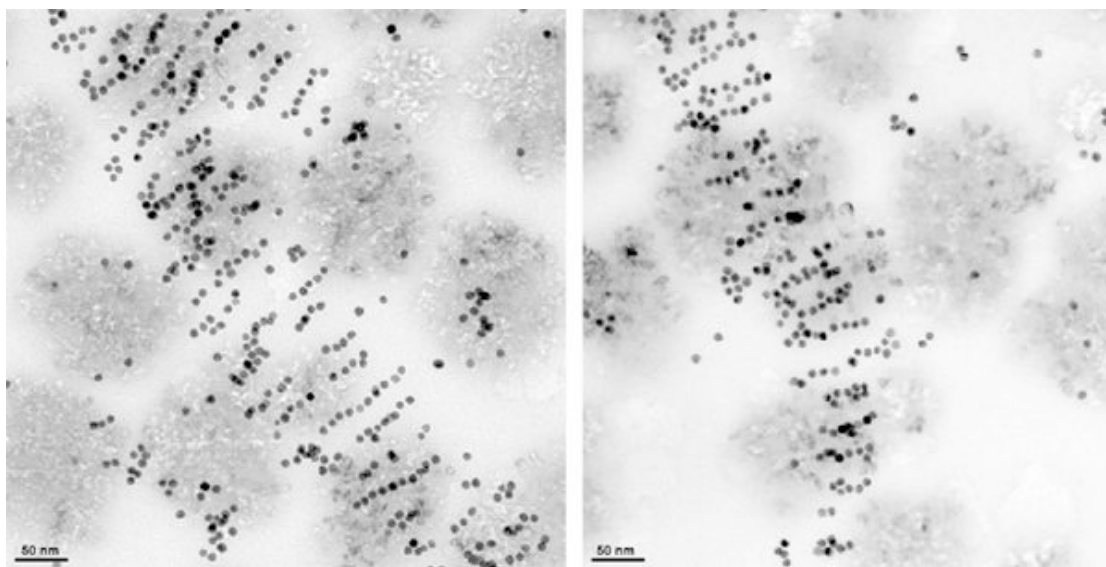


Table S1. Table showing statistical analysis of different conformations of DNA tubes annealed with different sized AuNPs. One hundred tubes are randomly counted and analyzed from non-overlapping images for each sample.

Sample	Type of DNA tubes	Percentage	Diameter (nm)	Number of nanoparticles	Angle	Periodicity
5 nm + Loop	Ring	29	66 ± 12	17 ± 4	–	56 ± 4
	Single spiral	59	97 ± 27	25 ± 6	32 ± 8	60 ± 4
	Double spiral	8	148 ± 28	41 ± 7	46 ± 8	60 ± 7
	Nested spiral	4	–	–	–	–
5 nm	Ring	55	58 ± 18	11 ± 1.7	–	56 ± 2.4
	Single spiral	45	80 ± 10	18 ± 2	40 ± 5	62 ± 3
10 nm	Ring	92	33 ± 12	9 ± 2	–	50 ± 2.4
	Single spiral	8	65 ± 8	17 ± 2	43 ± 4	57 ± 3.6
	Double spiral	1	143	34	59	–
15 nm	Ring	82	36 ± 12	8 ± 1	–	58 ± 8
	Single spiral	15	67 ± 18	14 ± 3	45 ± 12	61 ± 4
	Double spiral	3	177 ± 52	30 ± 6	57 ± 4	63 ± 6

It can be observed from the table that:

1. The spiral tubes generally have a larger mean tube diameter and wider size distribution than the stacked ring tubes, i.e. more tiles are needed to enclose one circumference of the tube. The fewer number of nanoparticles on each ring as compared to one period of a spiral tube also supports this difference in diameters.
2. The periodicities observed are generally smaller than the anticipated 64 nm when the tiles are all closely packed in parallel, which indicates that the tiles are rather distorted and expanded sideways and perpendicular to the axis of the tube due to the presence of the particles.
3. The angles measured for the single spiral tubes are larger for tubes with larger particles, this is consistent with the smaller diameter of the tubes.